Spring 2021

Composite-based additive manufacturing applications in the polymer injection molding cycle

Cody Bivens

Department:

COMPOSITE–BASED ADDITIVE MANUFACTURING APPLICATIONS IN THE POLYMER INJECTION MOLDING CYCLE

by

CODY MICHAEL BIVENS

A THESIS

Presented to the Graduate Faculty of the

MISSOURI UNIVERSITY OF SCIENCE AND TECHNOLOGY

In Partial Fulfillment of the Requirements for the Degree

MASTER OF SCIENCE IN AEROSPACE ENGINEERING

2021

Approved by:

Dr. K. Chandrashekhara, Advisor
Dr. Jillian Schmidt
Dr. Lokesh Dharani

ABSTRACT

The experimental method utilized in this research was the application of composite-based additive manufacturing (CBAM) mold plates in the injection molding process. The mold plates comprised carbon fibers and polyether ether ketone (PEEK) matrix. Modifications were made to the mold plates post manufacturing in order to properly adapt to the rest of the injection molding die. A custom cooling system was engineered and integrated into the injection molding machine for the CBAM mold plates. The polymer processed in the injection molding cycle for this study was Lustran 348 acrylonitrile butadiene styrene (ABS). The result of the trials conducted in this research demonstrated that polymer injection molding with CBAM mold plates was feasible and comparable to metal molds. However, adverse effects noted from using these parts made via the CBAM mold plates were rougher surface finishes and high adhesion between the polymer/tooling surface interface. In fact, the adhesion was so great that upon removal of the part from the mold, some regions of the PEEK matrix were torn from the tooling surface leaving a visibly unsmooth manifold behind. Further research and applications of CBAM mold plates could demonstrate promise in replacing the expensive, subtractive computer numerically controlled (CNC) metal mold plates for relatively small cycles.

ACKNOWLEDGMENTS

I would like to thank my academic advisor Dr. K. Chandrashekhara for his invaluable guidance and leadership. He instilled a sense of purpose, direction, and motivation in me as a graduate research student. His encouragement to pursue research opened new avenues for my future.

To my advisory committee: Dr. Jillian Schmidt and Dr. Lokeswarappa Dharani, I thank you for being influential educators throughout both my undergraduate and graduate experiences here at Missouri University of Science and Technology.

Thank you Impossible Objects for the teamwork, collaboration, and funding of our experimental research in the injection molding process. This has been a very insightful and unique learning experience.

I would also like to thank our research team for being very accommodating, knowledgeable, and having a desire to achieve common goals. Their assistance throughout this process is very much appreciated.

Recognition is due for two of my closest "friends," Christopher Bates and Mason Bringus, for their "encouragement" to pursue research. These gentlemen were always there through senior design to the all-nighters we pulled to complete our projects in graduate school.

Last, but not least, I would like to thank my family and friends for their love and support throughout my academic career. Most importantly, my parents deserve as much recognition for always encouraging me to persevere.

TABLE OF CONTENTS

LIST OF ILLUSTRATIONS

LIST OF TABLES

1. INTRODUCTION

1.1. PURPOSE

Injection molding is responsible for most polymer components made in industrial settings. In fact, the injection molding process utilizes thermoplastics and thermoset polymers, glass, metals, and even other materials [1]. Some applications of injection molding products are water bottles, pens, eating utensils, casings for computer screens, and even the dental mounting plates that were provided by Gnathodontic Services, Inc. for this research, which are displayed in Figure 1.1 below.

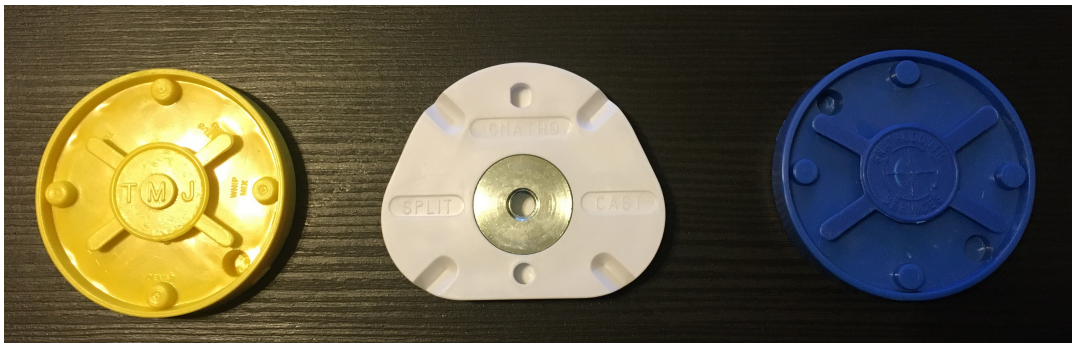

Figure 1.1: Thermoplastic Injection Molded Dental Mounting Plates

Injection molding with thermoplastics is a process where small, solid polymer pellets are converted to a viscous molten state and injected into a mold cavity with high pressure, taking the form of the cavity, and solidified as a whole part via a cooling process. Injection molding dies, which contain the entire assembly of platens, ejection pins, mold cavities, and other components, have traditionally required — often complex — subtractive CNC machining. Throughout various industrial applications, injection molding dies are subjected to numerous cycles — often in excess of one million [2]. As a result, machining a metal injection molding die becomes very costly, especially due to the high–precision machining the process necessitates. In more recent manufacturing, engineers have sought ways to create custom parts, or molds, with the intention of only subjecting the mold

cavity to a few hundred cycles, possibly fewer. The objective in this stage of injection molding is to determine a cost–effective and qualitative method to produce custom parts for orders requiring substantially fewer cycles than traditionally seen in mass–production industries.

One such proposition is the application of composite–based additive manufacturing. The idea is to design mold plates that would normally be manufactured via subtractive CNC machining and create the mold plates with composite materials as an alternative. Composites primarily comprise a fiber and a matrix material. For injection molding, the fibers provide the strength properties necessary to overcome the clamping and high injection pressures of the injection molding machine. Meanwhile, the matrix maintains the orientation of those fibers, transfers the loadings among the fibers, assists in maintaining the geometric profile, and establishes the quality of the surface finish of the composite mold plates.

CBAM methods provide the necessary capabilities to manufacture composite mold plates. Additionally, CBAM methods allow for quality complex mold geometries to be constructed in a manner similar to 3D printing at an affordable cost; whereas, traditional CNC machining implements a subtractive manufacturing method that results in excess material waste, expensive tooling wear and costs, and is typically only applied to isotropic materials [3]. Note that subtractive CNC machining is not strictly applied to isotropic materials; however, applying this manufacturing method to composites would very likely result in complete structural failure. Furthermore, CBAM mold plates can be designed and adapted to existing dies. Simply, the original metal mold plates are removed from the die and the CBAM mold plates are then fastened to the injection molding platens. This operation reduces the necessity to completely manufacture a new die for a new mold, which results in substantial time and manufacturing cost reductions. To better understand the layout of the injection molding machine and the die, refer to the proceeding section.

1.2. INJECTION MOLDING MACHINE

Injection molding machines are designed with four essential units. These units are the hydraulic power unit, the injection unit, the clamping unit, and the controls unit [4]. Within each of these units are mechanical and electrical components. Some components operate synchronously in their respective units, while other components operate in tandem. Together these units function to create parts inside of the injection molding machine. Some of the most critical components found in nearly every injection molding machine are displayed in Figure 1.2 below [5].

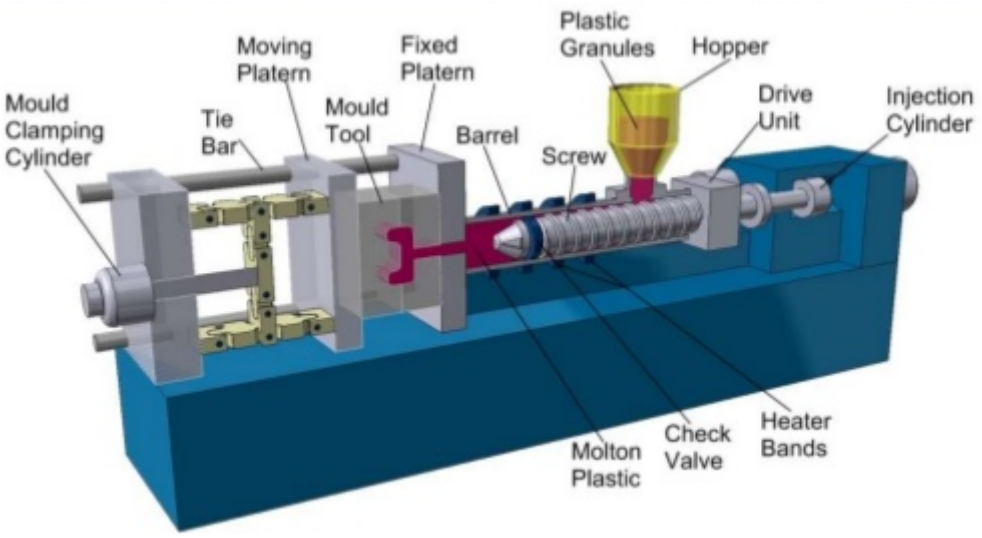

Figure 1.2: Injection Molding Machine Layout

Figure 1.2 above serves as a visual basis that displays some of the most critical components in the injection molding machine. Additionally, the units that house these components are examined in more depth in the proceeding subsections.

1.2.1. Hydraulic Power Unit. The hydraulic power unit is a system that contains components with the purpose of storing, pressurizing, moving, and conditioning oil. The reservoir where the oil is stored acts as the supply source for all machine functions. Near the reservoir is a breather that maintains atmospheric pressure inside of the tank. The atmospheric pressure is what initially forces hydraulic oil into the pumps. The pumps are then powered by an electric motor

that provides the necessary flow for various mechanical operations. Along these pumps exist several manifolds that contain internal porting to direct hydraulic oil to various valves. These valves direct the oil to specific machine components to accomplish a particular operation. On the return side of the hydraulic lines are filters to clean the hydraulic oil. Typically, there is a temperature gauge to monitor the oil temperature. The temperature of the hydraulic oil increases while cycling through the machine, which slightly decreases the viscosity of the liquid. To control the temperature of the hydraulic oil, the fluid is cooled by a heat sink that contains cavities. One cavity allows for the hydraulic fluid to enter; the other allows for water, or any coolant integrated into the system, to enter. Heat is then exchanged from the oil to the water through the cavity walls of the heat sink, thus cooling the oil [4]. However, a preset temperature for the hydraulic oil must often be reached prior to engaging the injection unit.

1.2.2. Injection Unit. The injection unit is a system that houses all of the components responsible for processing polymer granules into a molten state and extruding that molten material into the cavity of the injection molding plates for solidification. The polymer granules are poured into the hopper, or feeder, which is responsible for holding raw, unprocessed material. The hopper narrows to a region called the feedthroat that feeds polymer granules into the main component of the injection unit called the injection screw. This hopper-feedthroat assembly, as well as injection cylinders, are fastened to the feedthroat platen [4]. Within the feedthroat platen are cooling channels that prevent the polymer granules from melting prior to being placed within the barrel. The barrel serves as the housing of the screw. Next, there exists the injection platen with attached cylinder rods. The purpose of the cylinder rods is to move the injection platen forward and backward via hydraulic pressure. This movement of the injection platen induces linear actuation of the injection screw. Additionally, the injection screw rotates via torque provided by the hydraulic extruder motor [4]. This rotation of the

injection screw provides a shear loading to the polymer granules by scraping them between the screw and the barrel. This is the primary heat source for plasticizing the polymer. To assist in plasticizing the polymer, the barrel contains heater bands on the outside walls. Once the polymer is converted to a molten state, the polymer fills the end of the screw called the nozzle. This process is called creating a shot [1].

The shot provides the necessary volume of material to create the part, channeling, and cushioning for an injection molding cycle [1]. After the shot is created, the screw is actuated forward and the shot is extruded through the nozzle and into the cavity of the injection molding plates. Once the cavity is filled, the cooling system begins to solidify the part. The cooling system normally operates by passing coolant through the mold plates and exchanging thermal energy from the solidifying part via convective heat transfer. Simultaneously, the screw is retracted, more polymer granules are processed, and the shot is recreated for the next cycle. However, the next shot is not extruded until the clamping unit releases the previous solidified part.

1.2.3. Clamping Unit. The clamping unit is a system whose purpose is to open and close the mold, as well as to build tonnage [4]. The clamping unit contains two essential platens to which the mold is fastened. One half of the mold is fastened to the dynamic platen. The dynamic platen linearly actuates to open and close the mold. The other half of the mold is fastened to the static platen, which acts as a stationary object for the moving platen to build tonnage against. Towards the aft end of the clamping unit is the die height adjustment platen, which adjusts the clamp assembly for different mold thicknesses and the amount of tonnage applied to the static platen. The dynamic platen and the die height adjustment platen are connected via a toggle mechanism that helps to maintain tonnage during the injection cycle. On the rear side of the die height adjustment platen is a fastened clamp cylinder. The clamp cylinder bisects the

crosshead attached to the toggle mechanism. The crosshead is the mechanical coupling between the clamp cylinder and the toggle mechanism [4]. When the clamp cylinder is actuated forward, the toggle mechanism engages and closes the mold; when the clamp cylinder retracts, the toggle mechanism disengages and the mold opens. After the toggle mechanism disengages, the hydraulic ejector mechanism engages. This mechanism contains a hydraulic eject cylinder and a knockout bar [4]. When the hydraulic eject cylinder engages, the knockout bar is pushed forward. Ejector pins fastened to the knockout bar physically eject the solidified part from the mold. The operational parameters such as injection pressure, temperature, volume, velocity, clamping tonnage, cycle times, and others implemented in the injection molding cycle are normally user input values defined in the controls unit.

1.2.4. Controls Unit. The controls unit is the system that contains the computer hardware that operates the injection molding machine as well as the interface for user input. There are two main hardware assemblies integrated into the controls unit: the processor control assembly (PCA) and the operator station assembly (OSA) [4]. The PCA contains two essential sub-assemblies, which are the power supply and the card cage. The power supply has two functions: convert alternating current to direct current and supply power to the motherboard [4]. The motherboard houses all of the necessary computational components for machine operation, as well as the connectors linked to the OSA. The OSA is the user interface to the control unit. Here the user can control all machine functions from the electric motor of the hydraulic power unit to the injection unit's processing parameters and the clamping unit's applied tonnage to the static platen. Figure 1.3 displays most of the main components utilized in this research to produce plastic parts via the polymer injection molding process.

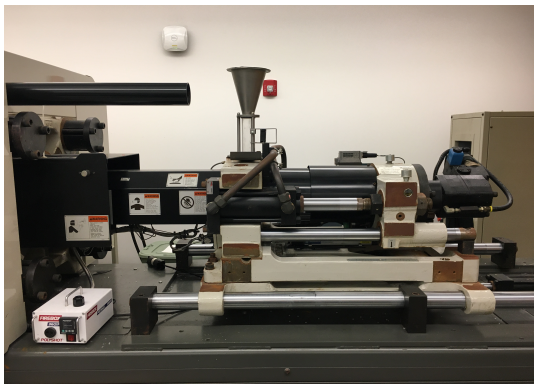

(a) Injection Unit

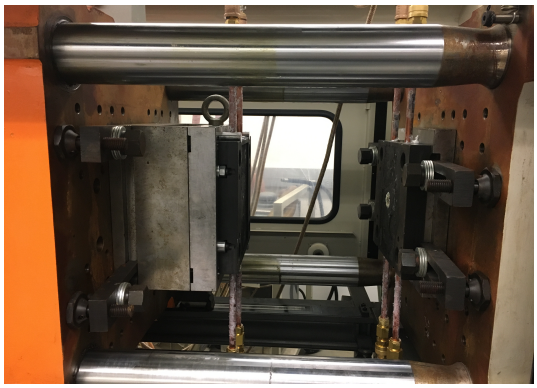

(b) Injection Molding Die

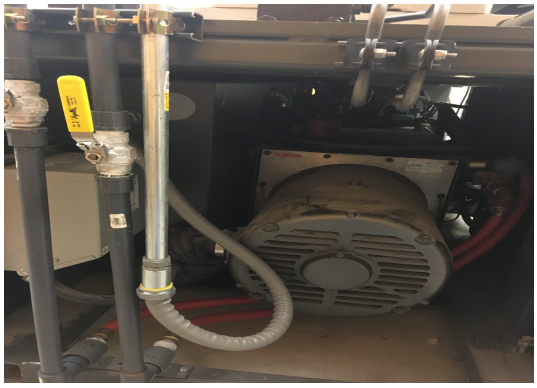

(c) Hydraulic Power Unit

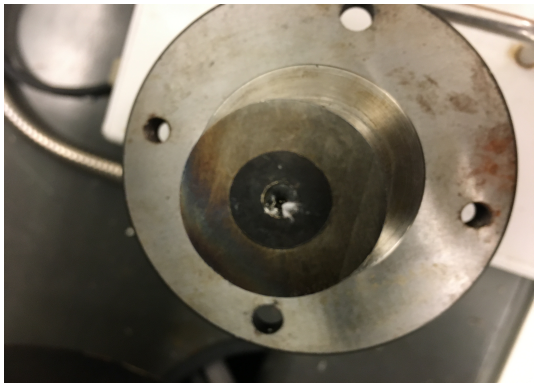

(d) Heated Sprue Bushing

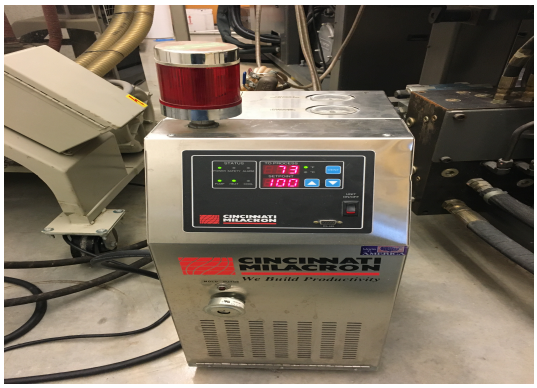

(e) Thermal Controller

(f) Polymer Dryer

Figure 1.3: Injection Molding Machine Systems

1.3. POLYMERS

1.3.1. Description. A polymer is defined as a material containing large molecules whose physical compositions contain linked multiples of simpler chemical units [1]. Polymers can be found throughout nature or fabricated synthetically. For example, DNA structures, proteins, and silk are examples of naturally occurring polymers; whereas, rubber, 3D printing filaments, and graphene are examples

of synthetic polymers. Many synthetic polymers are created in laboratory settings via a process called polymerization [6]. The process usually consists of combining natural and/or synthetic materials with heat, pressure, and a catalyst. This process forces the monomers from various materials to break and form new synthetic bonds with each other.

The morphology of plastic polymers normally are either amorphous or semi-crystalline. The orientation of amorphous polymer chains contain disorder and random packing orientations. As a result, amorphous polymers have a glass transition temperature, but not a set melting temperature. However, semi-crystalline polymers have both a glass transition temperature and true melting temperature because the the orientation of the polymer chains are more organized and packed together [1]. One important note is that due to chemical compositions, moisture content, and other environmental factors the temperatures for melting and glass transition would be more appropriately viewed as a range of values.

1.3.2. Acrylonitrile Butadiene Styrene. One important example of a polymer utilized in this research is ABS plastic. Examine the polymerization process of ABS. First, the composition of ABS plastic is three synthetically bonded monomers: acrylonitrile, butadiene, and styrene. Acrylonitrile is a synthetic product from the reaction of ammonia and propylene. This monomer provides chemical resistance and heat stability for the polymer. Butadiene is a synthetic by–product from heated ethylene production. This monomer provides toughness and impact resistance for the polymer. Styrene is a synthetic material that is manufactured from dehydrogenating ethyl benzene. This monomer provides rigidity and the ability for ABS to be processed. Since these monomers do not naturally mix, a process called emulsion is applied and the monomers are combined to form ABS polymer chains [7]. The molecular structures of the monomers and polymer as well as the chemical formula are displayed in Figure 1.4.

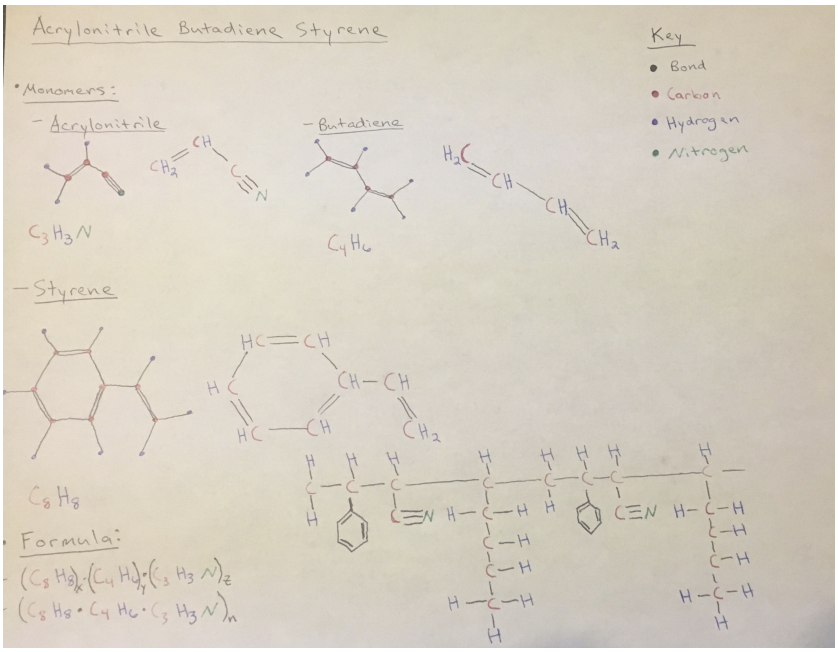

Figure 1.4: Chemical Composition of ABS Polymer

1.3.3. Processing Methods of ABS. ABS granules appear as small, cream colored pellets when synthesized. After being synthesized, there are a few methods in which ABS is typically processed. Two of those methods are injection molding and extrusion. The latter method has applications in 3D printing parts. Figures 1.5a and 1.5b display the raw material variations of ABS for injection molding and extrusion, respectively. The filament winding in Figure 1.5b has had black dye added to the ABS polymer; whereas, Figure 1.5a has not received any post–production modifications. Figure 1.5c and Figure 1.5d display parts that were manufactured via injection molding and extrusion, respectively. Although ABS may also be processed by other methods, this research will primarily focus on injection molding.

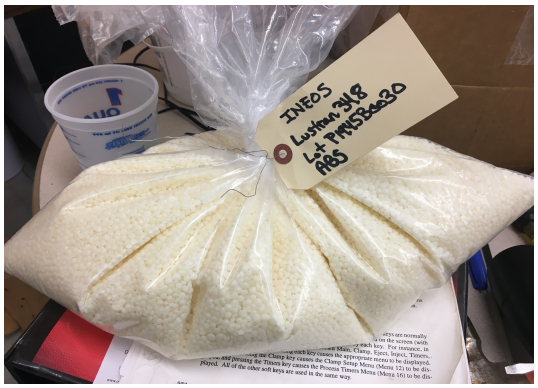

(a) Polymer Granules for Injection Molding

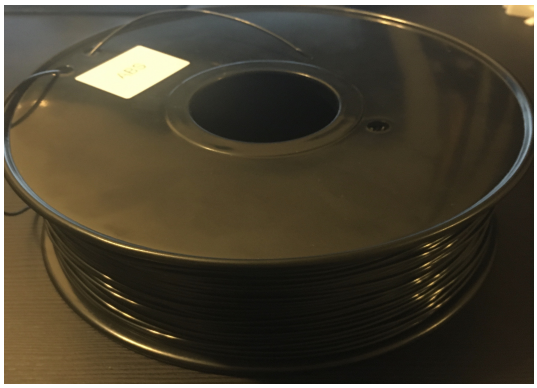

(b) Filament Winding for 3D Printing

(c) Injection Molded Controller

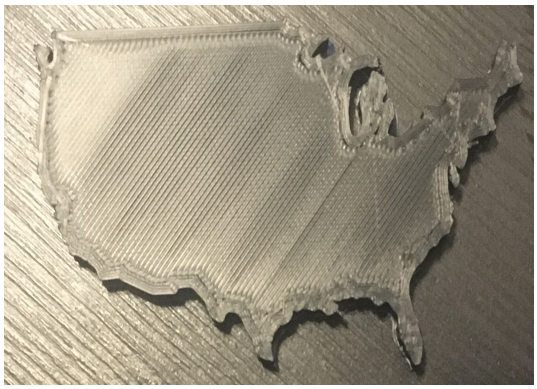

(d) 3D Printed Part

Figure 1.5: ABS Polymer and Applications

2. MOLD PLATES

This research of CBAM applications to the injection molding process is funded by Impossible Objects. This company manufactured injection molding plates via the CBAM method and subtractive CNC post-processing methods. Further post-processing of the mold plates was determined and machined upon arrival at Missouri University of Science and Technology.

The laboratory that is reserved for this research is located in Toomey Hall at Missouri University of Science and Technology. In the laboratory is a Cincinnati Milacron VT 165 polymer injection molding machine, the controller for the heated sprue bushing, the coolant thermal controller, the dryer for the polymer pellets, proper storage bins for raw materials, the validated user's manual, and proper safety and emergency shut-off protocols.

The material processed via injection molding for this research was Lustran 348 ABS. This material was chosen because the substance's processing parameters best adapted to the injection molding machine with respect to other provided materials. Future research may utilize other polymers, such as low density polyethylene or polypropylene.

2.1. SUBTRACTIVE CNC MACHINING

2.1.1. Process. Injection molding plates contain the cavity that is injected with molten polymer to create plastic parts. This cavity is normally created via subtractive CNC machining; pre-programmed computer software navigates factory tools and machinery to mill and tool metal base blocks into the final mold plates. This subtractive machining method provides the necessary channeling for the molten polymer to fill the part volume.

The molten polymer created to form the shot must fill the entire cavity volume of the mold plates. This includes the channeling (sprue, runners, and gates) and parts. The sprue is the opening to the injection mold through which

molten polymer flows. Next, the material is directed to various locations in the mold cavity via runners. At the end of the runners are gates, which are the location sites for the part cavities. Material flows through the gates and completely fills the parts, gates, runners, and sprue for a successful shot.

2.1.2. Applications. Initially, the polymer injection molding die in this research contained mold plates that were manufactured by subtractive CNC machining methods. The cavity of these mold plates is located entirely in the dynamic mold plate. The mold cavity is an extruded cut containing the outline of a rectangle with filleted corners. The dimensions of the cavity used to create plastic parts are 9.8125 in. of length, 5.1875 in. of width, 0.125 in. of depth, and a 0.25 in. radius for the filleted corners. There are five ejector pin sites located in the tooling cavity. Figure 2.1 below displays the metal mold plates.

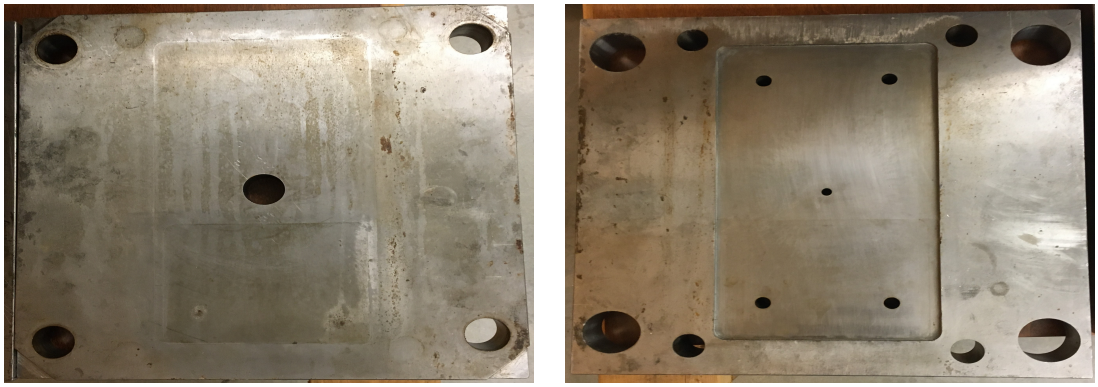

(a) Metal Static Plate (b) Metal Dynamic Plate

Figure 2.1: Metal Mold Plates

Although the exact metal of the metal mold is unknown, the most common material used for injection molding plates in industry is P20 steel [8]. Therefore, P20 steel will be the material utilized for the metal mold analysis. Pertinent properties of P20 steel pertaining to this research are displayed in Table 2.1 below.

Table 2.1: P20 Steel Properties

P20 Steel Properties		
Density	0.284	lb/in^3
Tensile Strength	125	ksi
Compressive Strength	125	ksi
Elastic Modulus	29,700	ksi
CTE, linear	7.1	µin/(in-°F)
Thermal Conductivity	24	BTU/(hr-ft-°F)
Poisson's Ratio	0.3	-

2.1.3. Advantages. CNC milling and tooling of metal base blocks allows for machining with high precision and accuracy. As a result, intricate molds can be machined with very smooth surfacing. Also, metal mold plates can be threaded, which allows for the integration of more efficient coolant systems. Heat transfer during the milling and tooling process can be easily controlled with coolants such as water. Since metal materials are isotropic, the induction or reduction of thermal energy will cause the metal to thermally strain equally in all directions. Commonly used metals for injection molding have high strengths, which is why metal mold plates are able to withstand the high injection pressures and clamp loadings induced during the injection molding cycle.

2.1.4. Disadvantages. However, creating the channeling and parts from subtractive methods often requires expensive CNC machining. The machining time for an injection molding die can take from weeks to months, as well. Although these molds may be subjected to more than a million cycles, some molds may not necessitate such numerous cycles. For example, a consumer may desire a custom part that only demands a few hundred reproductions. Producing a metal mold for an order of this small magnitude would likely not be cost effective. One solution that may reduce the manufacturing cost of mold plates is through composite–based additive manufacturing.

2.2. COMPOSITE–BASED ADDITIVE MANUFACTURING

2.2.1. Process. CBAM is a type of sheet lamination that builds objects from a composite material. The CBAM process for creating injection molding plates is performed in a series of steps. First, a computer–aided design (CAD) model of the mold plates is inserted into a slicing software to be simplified into horizontally sliced layers. Each of these layers is digitally mapped and encoded instructions are created for a printing machine to physically reproduce each individual layer. The printing machine uses a wetting fluid to print in accordance with the encoded instructions for that digitally mapped layer. Then, the printed sheet is covered with a powder–based thermoplastic-polymer [3]. Adhesion occurs at the fluid-powder interface, while the remaining loose powder is removed by a vacuum. The result is called a page. The cycle repeats with the next page being stacked upon the previous. This cycle is repeated until all pages are created. The completed set of pages is called a build block, not a book. The build block is then fused via heat and compression [3]. Heating melts the powder and fuses the sheets. Compressing the build block presses the fibers of the composite into a solid mass; thus reducing the height of the build block to the appropriate size of the finished object [3]. Lastly, post–production methods are applied to the object to produce the mold plates. Figure 2.2 below displays the outlined process.

2.2.2. Applications. The CBAM method was implemented to create carbon fiber/PEEK mold plates for this study. Relevant properties of carbon fiber/PEEK pertaining to this research are displayed in Table 2.2 below [9, 10, 11]. These composite mold plates were designed to replace the metal mold plates originally manufactured with the injection molding die. After the composite mold plates were created, subtractive manufacturing methods had to be implemented in order to prepare the mold plates for installation to the injection molding die.

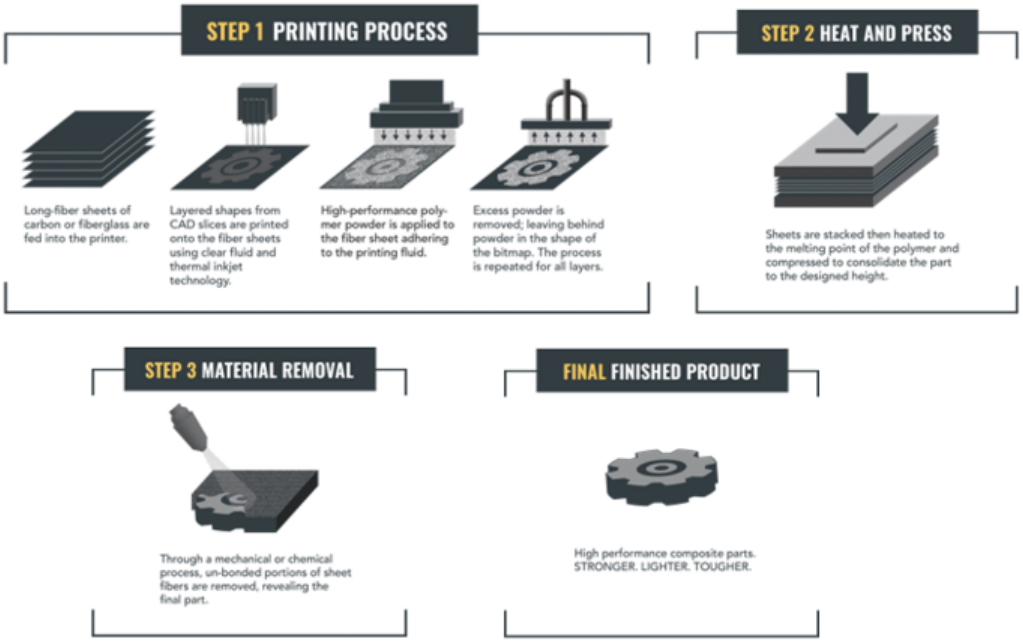

Figure 2.2: Additive Manufacturing Using CBAM Method

Table 2.2: Carbon Fiber/PEEK

Carbon Fiber/PEEK		
Nominal Fiber Volume Fraction	0.22	-
Density	0.0506	lb/in^3
Tensile Strength	19.1	ksi
Compressive Strength	23.5	ksi
Elastic Modulus	1,848	ksi
CTE, xy-Linear	7.0	µin/(in-°F)
CTE, z-Linear	36.4	µin/(in-°F)
Thermal Conductivity	0.16	BTU/(hr-ft-°F)
Poisson's Ratio	0.32	-

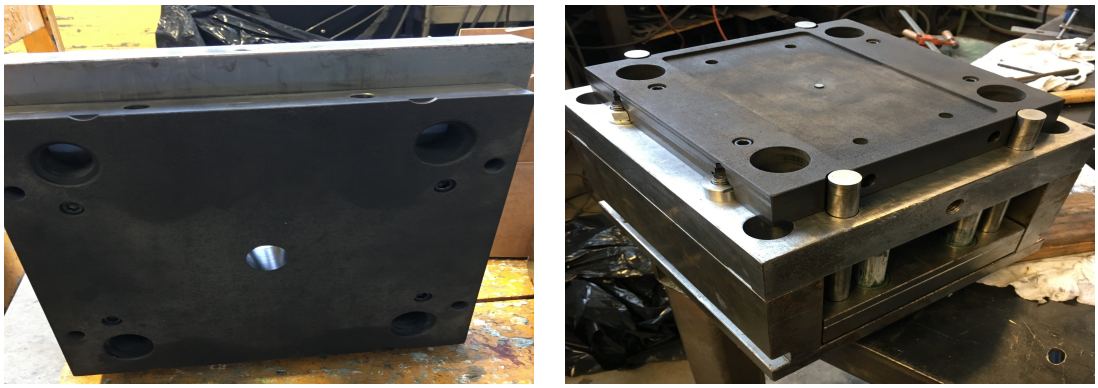

(a) Static Plate (b) Dynamic Plate

Figure 2.3: CBAM Mold Plates Fastened to Injection Molding Die

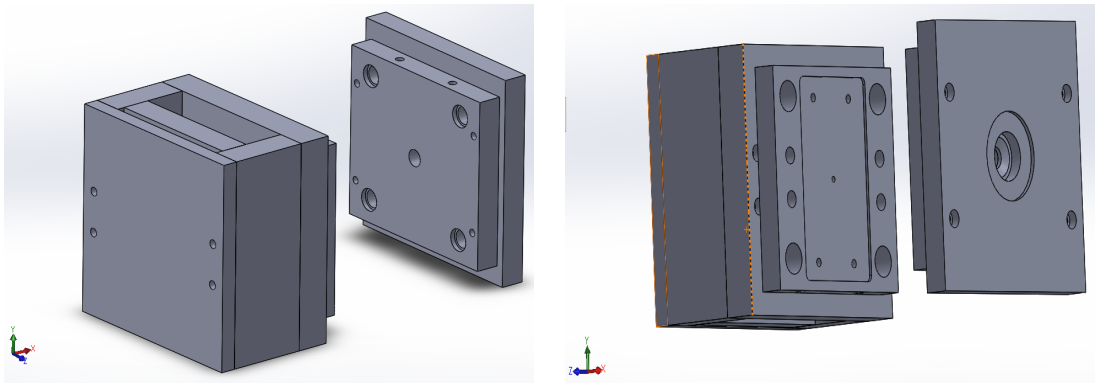

(a) Static Plate View (b) Dynamic Plate View

Figure 2.4: CAD Model of CBAM Mold Plates

The dimensions of the CBAM mold plates differed from the metal mold plates due to manufacturing limitations of the CBAM printing space. Specifically, the dynamic mold plate was 10 in. of length, 10 in. of width, with 1.375 in. of depth and the static mold plate was 11 in. of length, 10 in of width, 1.375 in. of depth. The mold cavity has the same dimensions as reported for the metal mold. Additionally, there are five ejector pin sites located within the mold cavity. Similarly to the metal mold, the CBAM mold cavity is contained entirely within the dynamic mold plate. The surface area surrounding the cavity of the dynamic plate, SA, is the region that tonnage is applied through to the static plate.

The composite has a compressive strength, σ_c, of 23.5 ksi. In order to determine the maximum tonnage, P_{max}, that the CBAM mold plates can experience without yielding, Equation (1) is utilized:

$$P_{max} = \frac{\sigma_c * SA}{2000lbs} \tag{1}$$

Applying the appropriate values to Equation (1) produces the following:

$$P_{max} = \frac{23,500psi * 41.125in^2}{2000lbs} \approx 483tons$$

The maximum applied tonnage that the plate can withstand is 483 tons. This tonnage far exceeds the injection molding's tonnage limits, which is 165 tons; therefore, the CBAM mold plates will withstand the total applied force from the clamping unit and no tonnage modifications need to be made to the clamping unit.

However, a few modifications had to be made to the CBAM mold plates post manufacturing. The first modification was applied in order to integrate a coolant system within the mold plates. Machinists had to bore 0.5 in. holes centered halfway through the thickness of the plates from the top to the bottom. This process required great care and caution because the boring process risked inducing delamination, excess fiber exposure, or cracking the plates.

For the half of the die containing the static plate, a machinist bored a hole through the front face for the heated sprue bushing. This provided the necessary channeling for injection into the cavity. Four additional holes were bored into the front face to allow for flange bushings and $\frac{5}{16}$ in. diameter bolts to be fed

through the CBAM plate and fastened to the metal platen. Notice in Figure 2.3a that, excluding the injection site, there appear to be eight bored holes. Four of the flange bushing locations were originally manufactured via the CBAM process. However, after manufacturing the CBAM mold plates experienced slight thermal shrinkage. Therefore, these holes were slightly misaligned and four new locations for the flange bushings needed to be machined for the static plate and the metal platen.

The other half of the die containing the dynamic plate necessitated a few modifications in order to be installed to the dynamic platen. The effects of thermal shrinkage, although small, had greater effect on this mold plate. First, only one of the five ejector pin sites matched those manufactured for the mold plate. To resolve this issue, the middle ejector pin was aligned with the ejector pin site of the mold plate and the other four ejector pins were removed. In order to prevent these exposed ejector pin sites from clogging with polymer during the injection process, a filler that could adequately withstand the temperature and pressure of the molten polymer needed to be applied. Specifically, the material needed to be able to withstand temperatures near 500°F and withstand injection pressures of at least $1,800$ psi. A variant of steel–reinforced epoxy formulated by J–B Weld produced a yield strength of $5,020$ psi and had the ability to withstand temperatures up to 550°F [12]. So, this variant of J–B Weld was used to fill these four ejector pin sites. The process required 6 hours for setting and 24 hours for the material to cure [12]. Next, four holes were bored through the front facing of the dynamic plate and the metal platen to allow for flange bushings with $\frac{5}{8}$ in. diameter bolts to be installed. Then, four additional holes were bored near the exterior of the metal platen to allow for bushings and bolts to be inserted. This modification serves two purposes: the first is the hold the metal platen components together, the second is to act as a support to restrict any motion of the CBAM mold plate. Lastly, an $\frac{1}{8}$ in. diameter by $1\frac{3}{4}$ in. depth bored hole was installed in the center

of the through-thickness face, halfway between the center of the coolant lines for thermocouple installation. For a complete visual of these modifications refer to Figure 2.3b.

2.2.3. Advantages. The CBAM method is superior to other alternative methods, such as 3D printing, for several reasons. To start, objects can be created faster with the CBAM method. Objects can also be created from a wider range of materials. The material properties of CBAM objects have greater advantages, especially with respect to strength. Furthermore, issues commonly found in 3D printing, such as shrinkage and warping, can be eliminated with the CBAM method [3].

CBAM molds are significantly cheaper to fabricate than metal molds. Metal molds tend to average around $\$12,000$ [13]; whereas, the CBAM static and dynamic mold plates cost \$640 and $\$1,090$, respectively. The total cost of $\$1,730$ is less than 15 percent the cost of a metal mold. For small production cycles, the cost savings with CBAM molds is substantial.

There is significant weight reduction when using CBAM molds over metal molds. According to the Solidworks mass properties feature, the volumes of the CBAM static and dynamic plates are 187.17 $in.^3$ and 109.58 $in.^3$, respectively [14]. Multiplying by the reported density of this carbon fiber/PEEK variation approximately yields weights of 9.5 lbs. and 5.5 lbs., respectively. While the metal mold plates used in this study do have a larger geometry that more appropriately configures to the injection molding die, the comparison will reduce bias by taking the same volume of the CBAM molds and multiplying by the density of P20 steel. Referring to Table 2.1, the density of P20 steel would yield respective weights of 53.2 lbs. and 31.1 lbs. The combined weight of the CBAM mold plates is approximately 18% of the P20 steel mold plates with respect to the same volume. This weight savings allows for easier mobility, reduces shipping costs, and reduces the need for some installation equipment.

While the manufacturing times for metal injection molding plates can take several weeks, the manufacturing time for the CBAM mold plates allows for orders to be fabricated, shipped, and received within the same work week. Table 2.3 displays the production times to manufacture the CBAM mold plates.

Table 2.3: Production Times of Carbon Fiber/PEEK Mold Plates

Production Time for CBAM Mold Plates		
Print Time	12	(hrs)
Bake Time	12	(hrs)
Post-Processing Time	2	(hrs)
Total Time	26	(hrs)

2.2.4. Disadvantages. CBAM mold plates are more difficult to fabricate with precision and accuracy than metal mold plates. The composition of the CBAM mold plates comprises fibers and a binding matrix, so the final part does not display isotropic properties. One important note is that there are special circumstances where a composite may demonstrate isotropic properties. For example, randomly oriented short-chopped fibers in a binding matrix may be characterized as isotropic [15]. However, CBAM mold plates are not made with randomly oriented, chopped fibers in three dimensions; thus, the composite displays some anisotropy. Specifically, CBAM mold plates display transverse isotropic properties [3]. Therefore, when heat is applied to the CBAM mold plates during the injection process, the mold plates will expand differently in the through–thickness direction than the planes parallel to the tooling surface. Also, these composite plates are porous and must avoid contact with fluids; therefore, special cooling systems have to be integrated into the injection molding machine.

3. COOLANT SYSTEM

3.1. METAL MOLD PLATES

Coolant systems for traditional injection molding machines normally integrate coolant, coolant lines, valves, thermal processing unit, hoses, and threaded piping. Valves that open and close within the coolant lines are engaged to allow coolant — normally water — to flow. The coolant is then sent to a thermal processing unit, which is a machine that most often heats the coolant to a user–defined temperature. Then, the coolant travels through a network of hoses, fittings, and threaded metal piping. The threaded metal piping is screwed into the threaded metal mold plates. The threads in the mold plate allow the coolant to experience direct convective heat transfer from the mold plate. The coolant enters the mold plate via the inlet channel and exits via the outlet channel. Finally, the coolant leaves the system via the return line. The integrated coolant system consumes thermal energy from the mold plates, thus cooling the molten polymer and allowing the part to solidify in the mold prior to ejection. Figure 3.1 displays disconnected threaded quick connects that are normally screwed into the metal mold plates. Attached to the upper ends of each component is a cut portion of the coolant hosing prior to replacement.

Figure 3.1: Threaded Piping with Quick Connects for Coolant System

An important note is that initially the coolant is heated in order to heat the mold plates to the desired initial condition. However, the molten polymer is usually a few hundred degrees hotter than the mold plate. Therefore, after the first shot, the mold plates are no longer being heated; the mold plates are being cooled. The purpose for initializing the mold plates to a hotter temperature than the preprocessed coolant is important. A few reasons this is practiced is to prevent some polymers from crystallizing prior to complete injection, prevent warping of the part, and allow the desired properties of the polymer to be exhibited in the part that may otherwise be altered due to high thermal gradients [16].

3.2. CBAM MOLD PLATES

3.2.1. Limitations. The CBAM mold plates contain bored cooling channels similar to those found in the metal mold plates. There are a few limitations that must be considered with these cooling channels of the CBAM plates. First, threading composites is advised against because this process risks inducing delamination and possibly cracks within the plates. Next, while the bored cooling channels have a smooth internal surface, there are exposed carbon fibers present. Also, the composite's matrix exhibits a porosity, so the coolant needs to avoid direct contact with the mold plates in order to avoid inducing damaging hygroscopic effects. Next, the CBAM plates are transversely isotropic, so the thermal expansion coefficients differ between the in-plane and through-thickness of the plates. Therefore, when the mold plates experience thermal strain, the shape of the bored holes will experience a change in eccentricity. Lastly, carbon fiber/PEEK is not as thermally conductive as metals. So, heating and cooling the CBAM mold plates will take longer than what is normally expected in the injection molding process.

3.2.2. Corrosion. The literature will temporarily digress to discuss corrosion cells and the Galvanic Series; corrosion is a common issue in metallic mold plates and metallic coolant systems. A corrosion cell requires four components: an

anode, a cathode, an electrolyte, and a metallic path. Corrosion may be induced by various methods and can be very destructive to expensive parts, especially injection molding plates [17]. The most critical method found in this study is galvanic corrosion.

Galvanic corrosion occurs when two dissimilar metals are in contact with each other and an electrolyte. In an active corrosion cell, the least electronegative material is the anode and the most electronegative material is the cathode. In the galvanic corrosion cell, the anodic metal sacrifices electrons to the cathodic metal at a rate that is dependent on the voltage induced between the two dissimilar metals and other environmental factors. The anode then corrodes, and as a result the cathode is protected. Figure 3.2 below displays the Galvanic Series, which provides the electronegativities of common metals and alloys [18]. This information may be utilized to determine the anode and cathodes in a galvanic corrosion cell.

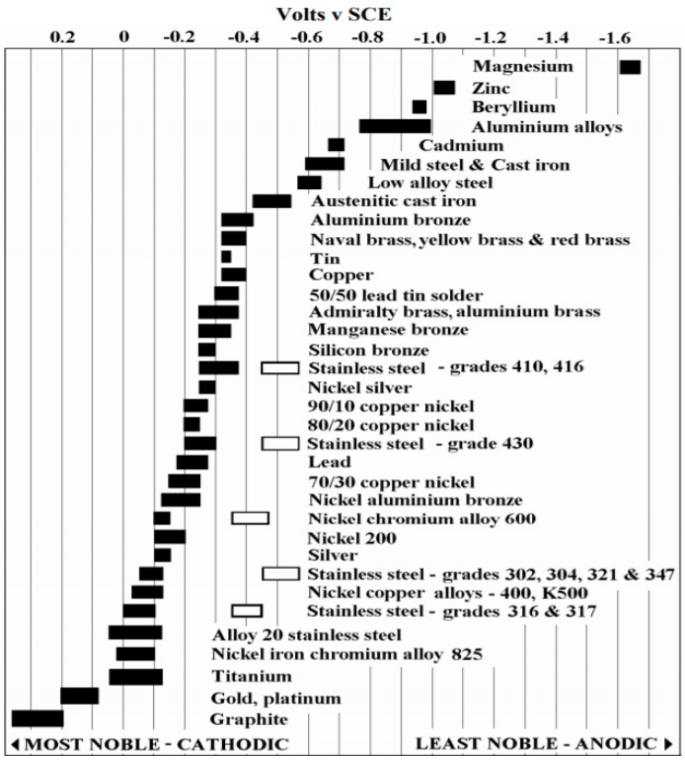

Figure 3.2: Galvanic Series

3.2.3. Solution. Since the cooling channels cannot be threaded, cooling pipes with high thermal conductivity will need to be inserted through the channels. This installation simultaneously eliminates damaging hygroscopic effects. Since metals typically are characteristic of high thermal conductivity, the pipe material choice will be metallic. Conductive heat transfer will occur at the interface of the pipes and cooling channel walls, and convective heat transfer will occur between the coolant and pipes. However, because the thermal expansion coefficients of the composite and metal are likely to differ, the contact surface area of the pipe and cooling channel interface will slightly change; thermal expansion of the composite will change the eccentricity of the cooling channel. Coating thermal grease on the exterior of the surface of the pipes will assist with some of the lost thermal conductivity transmission. Also, the exposed carbon fibers in contact with the metallic pipes will produce an electronegative potential that will in turn induce a galvanic corrosion cell in the presence of an electrolyte, most likely moisture. Regardless of the metal chosen, the pipes are going to be anodic, meaning the pipes will corrode and the carbon fiber will be protected. However, the rate and significance of corrosion with respect to the other issues present will depend on the electronegativity of the chosen metal. The most appropriate solution of any of those presented above is the one that prioritizes the issue of the most urgency or severity.

The solution is essentially reduced to a problem that is two fold: select the optimal metal for heat transfer and corrosion resistance. The ABS–processing temperature is approximately 500°F for injection molding. In order to begin solidifying, the ABS needs to cool below the glass transition temperature, which is approximately 221°F [7, 19, 20]. Composite materials do not transfer thermal energy as quickly as metals typically. Since determining an effective and affordable method for producing custom parts is the objective of this research, solidification of the ABS part is of utmost importance. Additionally, the custom mold plates

are intended to be utilized for low–volume production. The CBAM mold plates will be subjected to substantially less corrosion throughout the tool's life cycle than the metal mold plates. Therefore, heat transfer will take precedence over corrosion and will be the primary motivator for selecting the appropriate metal. Table 3.1 below displays potential materials to be selected for the CBAM coolant system [7, 19, 20, 21].

Table 3.1: Material Data

Material Parameters			
Material	**Temperature (°F)**	**Thermal Conductivity (BTU/(hr-ft-°F))**	**Thermal Expansion (µin/(in-°F))**
Lustran 348 ABS	475-525	---	---
CF/PEEK	630	0.3	(7.0-36.4)
Type K Copper	400	400	16.8
Aluminum	350	237	23.1
Stainless Steel	750	15	17.8
Silicone HSC	500	0.55	(250-300)
Coolant (Water)	60-180	---	---
Air	---	0.0262	---

Considering that heat transfer is the primary objective of this task, type K copper appears to be the best choice. However, the injection temperature of the ABS polymer is approximately 500°F. The only material that meets the parameter of the injection temperature is stainless steel. However, the thermal conductivity of stainless steel is less than 4% that of type K copper. Furthermore, the temperatures reported in Table 3.1 are well below the actual respective melting temperatures of the metals. After consulting a thermodynamics expert, the conclusion was made that the temperature rating of the type K copper was likely reported to indicate the temperature at which the solder used to create a solder joint with the metal would fail. Since no solder joints were to be integrated into the cooling system, the type K copper satisfied the temperature parameter. The last parameter needing to be met with respect to the heat transfer issue was thermal expansion. The in-plane thermal expansion of the CBAM mold plates is $7.0\frac{\mu in}{in^{\circ}F}$. Type K copper is an isotropic material and will thermally expand at a

rate of $16.8\frac{\mu in}{in^{\circ}F}$ irrespective of the direction of measurement. This ensures that there will always be some contact at the pipe–to–cooling channel interface within the operating parameters of this study. However, observing the difference between the thermal expansion rates may create concern for stressing the cooling channel and potentially induce cracking. But, the through-thickness thermal expansion of the CBAM mold plate more than doubles that of copper and should thermally strain the mold plate cooling channels enough to avoid any excessively induced stress experienced from the expanding copper tubing at the pipe to cooling channel interface.

For the secondary problem of corrosion, Figure 3.2 should be consulted. The electronegativity values of copper, stainless steel, and aluminum fall within the same range of one another. Considering the carbon fibers have an electronegativity similar to graphite, the carbon fibers will be the most electronegative material presented in this study. So, there does not appear to be any substantial variance in electronegative potential among the anodic metals. This further supports the final choice to use type K copper as the design metal for the coolant system.

The silicone heat sink compound reported in Table 3.1 provides slightly better thermal transmission than air. So, the compound will be coated to the outside of the type K copper tubing to try to fill some of the void that becomes present between the copper tubing and cooling channel during thermal expansion. Regardless of the effectiveness, the silicone compound will also act as a lubricant for the copper tubing during installation to the cooling channels. The silicone compound displays non-Newtonian fluid properties and completely maintains form after shear stress is applied. This is important because the compound will be exposed to the porous regions of the composite's cooling channels. However, from a macroscopic observation, absorption of the compound by the composite does not appear to be a concern as the silicone can be easily wiped from the surface.

Microscopic effects of the silicone compound would need to be investigated in order to ascertain if any residual compound remains.

Type K copper tubing with $\frac{1}{2}$ in. outer diameter, $\frac{3}{8}$ in. inner diameter, and 18 in. of length was chosen. To connect the $\frac{1}{2}$ in. copper tubing to the rest of the coolant lines, a series of fittings and connections were selected. A custom pipe coupling was swaged onto the end of the copper tubing. On the other end of the coupling was a $\frac{1}{2}$ in. threaded female component. The threaded female component screwed onto a $\frac{1}{2}$ in. male quick release mechanism. On the other end of the quick release mechanism were $\frac{1}{2}$ in. male threads. A $\frac{1}{2}$ in. female pipe coupling was screwed onto these male threads. On the other side of the female pipe coupling was a $\frac{1}{2}$ in. male barb hose. The barb hose was inserted into the hose and fastened with a hose clamp. This process was repeated for all ends of each of the copper tubings, thus completing the circuit of the cooling lines. Figure 3.3 displays the description of the coolant system above that was integrated into the injection molding machine.

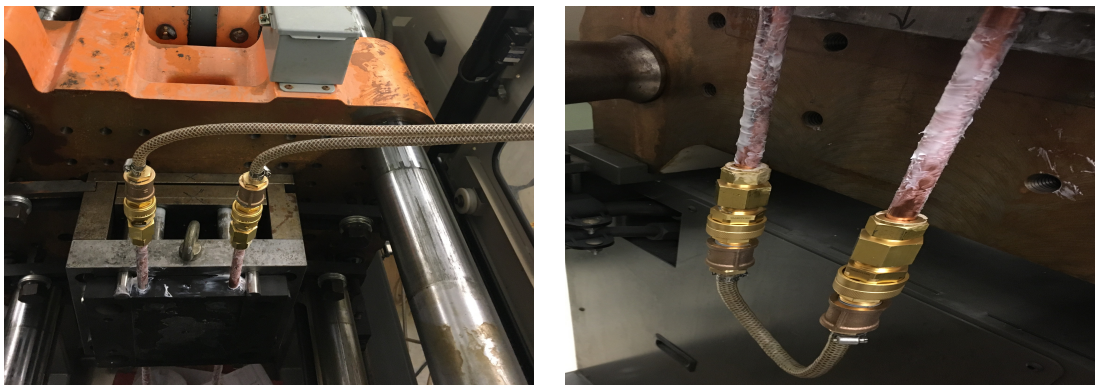

(a) Upper Portion (b) Lower Portion

Figure 3.3: CBAM Coolant System Assembly

4. ANALYTICS

The appropriate cycle times, such as injection, packing, holding, and cooling times, can be calculated analytically. However, these parameters can also be found via trial and error by selecting arbitrary cycle times and examining the part after production. Any defects in the part can likely be adjusted by altering the cycle time parameters. A paper presented during the International Conference on High Performance and Optimum Design of Structures and Materials derives the cycle time analytics for the injection molding cycle and will be heavily referenced here.

The cycle time is defined as the total time taken to inject the molten polymer into the cavity, pack the cavity in order to account for shrinkage during solidification, cool the molten polymer to solidify and gain rigidity, and finally eject the part from the mold. The cycle time is dependent on parameters such as injection fill, heat transfer, mold cavity volume, integrated ejection system, and more. The cycle time, T_{Cycle}, is defined via the following equation:

$$T_{Cycle} = T_{Filling} + T_{Packing} + T_{Cooling} + T_{MoldResetting} \tag{2}$$

Where,

$T_{Filling}$ is the time required to fill the part and channel cavities of the mold

$T_{Packing}$ is the time required to pack the fill to account for shrinkage

$T_{Cooling}$ is the time required to cool the part to complete solidification

$T_{MoldResetting}$ is the time allotted for actuating the dynamic mold plate and ejecting the part

4.1. FILLING

The total volume of the mold cavity is defined as the sum of the part and channeling volumes. This equation is displayed in more detail below:

$$V_{Total} = n(V_{Part}) + V_{Channeling} \tag{3}$$

Where,
n is an integer multiple of the defined cavity present within the mold

Often molds are designed to allow for multiple productions of one part per shot. But,

$$V_{Channeling} = n(V_{Runner} + V_{Gate}) + V_{Sprue}$$

So, the total mold cavity volume may be defined as:

$$V_{Total} = n(V_{Runner} + V_{Gate} + V_{Part}) + V_{Sprue} \tag{4}$$

Next, the volumetric flow rate for filling the mold cavity, $Q_{Filling}$, is given [22].

$$Q_{Filling} = \sum_{i=1}^{n} Q_{Part}(i) = nQ_{Part} \tag{5}$$

Where,

Q_{Part} is the part volumetric flow rate

Then, the required fill time is calculated by dividing the mold cavity volume by the mold cavity volumetric flow rate.

$$T_{Filling} = \frac{V_{Total}}{Q_{Filling}} \tag{6}$$

Or,

$$T_{Filling} = \frac{n(V_{Runner} + V_{Gate} + V_{Part}) + V_{Sprue}}{Q_{Filling}} \tag{7}$$

However, knowing the appropriate volumetric injection flow rate requires further investigation. For this injection system, the molten polymer is linearly extruded through a radial sprue bushing. This type of flow may be evaluated via the Hagen-Poiseuille equation for Newtonian fluids. Note that molten polymer flow is characteristic of non-Newtonian flow and requires correction following the proceeding derivation [22].

$$Q_{Filling} = nQ_{Part} \rightarrow \frac{dV(t)}{dt} = \frac{n\pi R_s^4 \Delta P_R}{8\mu(\dot{\gamma})L} \tag{8}$$

Where,

$\mu(\dot{\gamma})$ is the dynamic viscosity of the molten polymer

L is the specific length of the runners

R_s is the effective radius of the runners

ΔP_R is the pressure loss along the runners

Isolating the time differential in the following manner, the above equation can be integrated with respect to time bounded by 0 to $T_{Filling}$, and with respect to volume bounded by 0 to V_{Total}:

$$\int_0^{T_{Filling}} dt = \int_0^{n(V_{Runner}+V_{Gate}+V_{Part})+V_{Sprue}} \frac{8\mu(\dot{\gamma})L}{n\pi R_s^4 \Delta P_R} dV(t) \tag{9}$$

Evaluating the integral equation above:

$$T_{Filling} = \frac{(n(V_{Runner} + V_{Gate} + V_{Part}) + V_{Sprue})8\mu(\dot{\gamma})L}{n\pi R_s^4 \Delta P_R} \tag{10}$$

The dynamic viscosity of the molten polymer is a dependent function on the shear stresses to which the substance is subjected. Since molten polymer flow exhibits non-Newtonian characteristics, the shear rate of the fluid in the runners is modified in the following manner [22]:

$$\dot{\gamma}_s(r) = \frac{4Q_{Filling}}{\pi R_4} r \tag{11}$$

Where,

R is the actual radius of the runners, or the heated sprue bushing in this case

There is an intersection between the shear rate distributions of Newtonian and non-Newtonian molten polymers in laminar pipe flows. This intersection, or equivalency point, occurs at a nominal radius. So for this particular value of effective radius, the dynamic behavior of non-Newtonian fluid may resemble that of a Newtonian fluid. Considering this allows molten polymer flow to be modeled in accordance with the following equation [22]:

$$R_s \approx e_0 R \tag{12}$$

An empirical correlation can be established between the shear rate of non-Newtonian flow and viscosity; this is demonstrated in the following equations [22].

$$\mu = \frac{\mu_0}{1 + (\frac{\mu_0}{\tau}\dot{\gamma}_s)^{1-n}} \tag{13}$$

With,

$$\mu_0 = D_1 e^{\frac{-A_1(T_m - \bar{T})}{A_2 + (T_m - \bar{T})}}$$

Where,

A_1 and A_2 are material setting coefficients defined from the Williams-Landel-Ferry Equation and are valued at 17.44 and 51.6, respectively

D_1 is a material setting coefficient defined the Williams-Landel-Ferry Equation and must be solved for analytically, which can prove to be difficult

T_m is the temperature of the molten polymer at the injection location

$\bar{T}$ is the glass transition temperature of the polymer

τ is the critical stress level at the transition to shear thinning

n is the power law index in the high shear rate regime

To summarize, the dynamic viscosity is now modeled as a dependent function of the material composition of the polymer, the injection rate, and the geometry of the mold cavity.

4.2. PACKING AND COOLING

Next, the packing and cooling times are defined, $T_{Packing}$ and $T_{Cooling}$, respectively. The duration for packing and cooling is called remanence. Remanence is a very important duration in the injection molding cycle because most of the cycle's time occurs during this process and heavily influences the quality of the part as will be seen in this research. The packing and cooling times are defined via the following equations [22]:

$$T_{Packing} = \frac{d_{Gate}^2}{\pi^2 \alpha} ln\left(\frac{4(T_M - \bar{T}_W)}{\pi(\hat{T}_E - \bar{T}_W)}\right) \tag{14}$$

$$T_{Cooling} = \frac{d_{Sprue}^2}{\pi^2 \alpha} ln\left(\frac{4(T_M - \bar{T}_W)}{\pi(\hat{T}_E - \bar{T}_W)}\right) \tag{15}$$

Where,

α is the coefficient of thermal diffusivity of the molten polymer

d_{Gate} is the gate diameter

d_{Sprue} is the diameter of the sprue

$\bar{T}_W$ is the temperature of the mold plates

$\hat{T}_E$ is the temperature of the part upon ejection from the mold cavity

One important note is that the volume of molten polymer will experience shrinkage during the solidification process; therefore, the required times for packing and cooling will be slightly less than the values calculated via the prescribed equations above.

4.3. MOLD RESETTING

Lastly, the required time for the mold to open, the part to eject, and the mold to close to prepare for the next shot is calculated via the following equation [22]:

$$T_{MoldResetting} = 1.75 t_{dry} \sqrt{\frac{2D + 0.05}{L_M}} \tag{16}$$

Where,

t_{dry} is the time allotted for the part to dry

D is the maximum depth of the mold cavity

L_M is the clamp stroke length

This concludes the analytical derivation for the cycle time parameters. As stated previously, the cycle time values can be found experimentally if the analytics prove to be problematic for the user. However, some material data

sheets provide processing information pertaining to cycle times that eliminate the necessity to calculate these parameters. Regardless of the method that the cycle time parameters are obtained, these values can be implemented in experimentation and simulation.

5. EXPERIMENTATION

5.1. PROCESS

Products made via the injection molding process are called parts. The majority of parts that are made in industrial settings are from thermoplastic polymers, such as the ABS that is used to create parts in this study [1]. The preparation time for part manufacturing takes nearly an hour for the Cincinnati Milacron VT 165. User–defined parameters are initialized via the OSA of the controls unit. While most input parameters take immediate effect, the heating of the injection unit takes approximately 30 minutes. Temperatures set for the heater bands and the oil in the hydraulic power unit must be met before the controls unit will allow the user to actuate any part of the injection unit. After these temperatures are reached, the heating elements maintain these temperatures and the barrel begins a 30–minute soaking time. This soaking period helps to ensure that any residual polymer is processed and ready for ejection from the screw.

As previously mentioned, the ABS polymer granules are poured into a hopper that feeds the polymer into the hydraulic injection screw. The screw shears the polymer granules against the barrel wall. For the Cincinnati Milacron VT 165 there are three heater bands located on the exterior of the barrel that assist in processing the polymer. The temperatures at which these heater bands operate is user defined. For ABS plastic, the rear heater band is set at 465°F, the middle heater band is set at 475°F, and the front heater band is set at 485°F. The static injection molding platen has been fabricated for this machine to allow for the application of a heated sprue bushing. A heated sprue bushing is a critical component that helps ensure proper injection temperature and prevent clogging from occurring in the sprue. The heated sprue bushing is set at 485°F.

While material processing sheets recommend an injection pressure of $10,000$ psi. for ABS, the safety features integrated into this particular machine do not allow the machine to reach this pressure. Further restrictions on the injection

pressure are dependent on the allotted shot size, power provided by the hydraulic power unit, and other operational parameters. So, for producing parts within these mold plates the injection pressure is set to $1,800$ psi. When the processed molten ABS is injected into the mold cavity, approximately 98% of the cavity is filled with constant pressure. The remaining 2% is then filled with constant velocity [4]. After the cavity is completely filled, the pressure and velocity profiles of the injection cycle can be viewed by the user in the OSA.

Once the mold cavity is completely filled with molten ABS, the cooling cycle engages and begins to extract thermal energy from the ABS. After a set period of time, the molten ABS cools and solidifies, thus creating the part. The appropriate cooling time can be difficult to determine analytically. However, after a few trials the user can adjust the cooling cycle parameters to best fit solidifying the part. For the CBAM mold plates, thermal conductivity is nowhere near as effective as the metal mold plates. Therefore, the temperature that the coolant should enter the cooling channels needs to be set to a cooler temperature [2]. For the metal mold plates, the cooling temperature was set at 175°F. For the CBAM mold plates, the temperature was chosen at 100°F for this study.

After the cooling cycle time has passed, thereby solidifying the part, the clamping unit disengages and the part is ejected from the mold cavity. The next shot is created, the clamping unit engages, and the process is repeated. Important processing information pertaining to this study was captured from the OSA screen and is displayed in Figure 5.1.

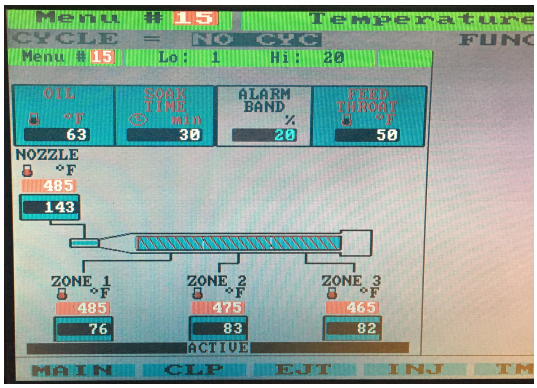

(a) Processing Temperatures

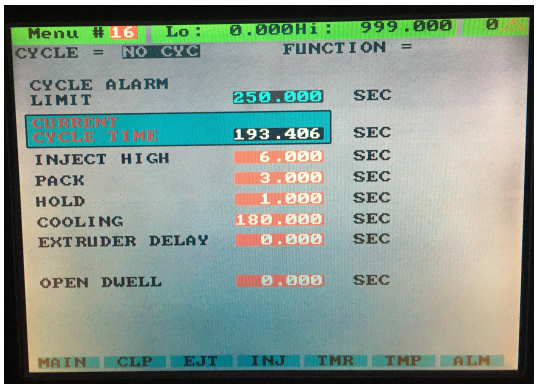

(b) Cycle Times

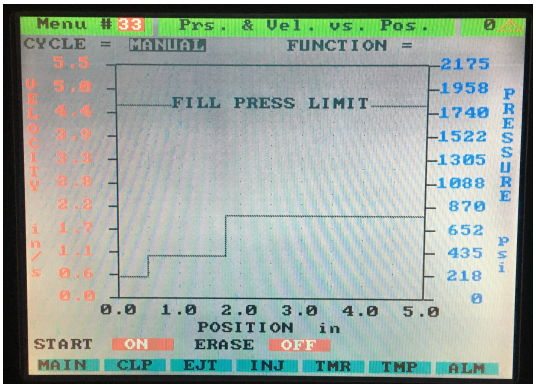

(c) Injection Profile

Figure 5.1: Injection Molding Processing Parameters

5.2. RESULTS OF ABS PART

Three trials were conducted in creating parts with the CBAM mold plates for this research. Each trial exhibited different results. After each trial, user input adjusted the cooling cycle parameters to help with solidification and part quality finish. However, further trials were discontinued due to tooling surface degradation. These trials are investigated in further depth below. The figures below display the results of the parts after removal from the CBAM mold plates.

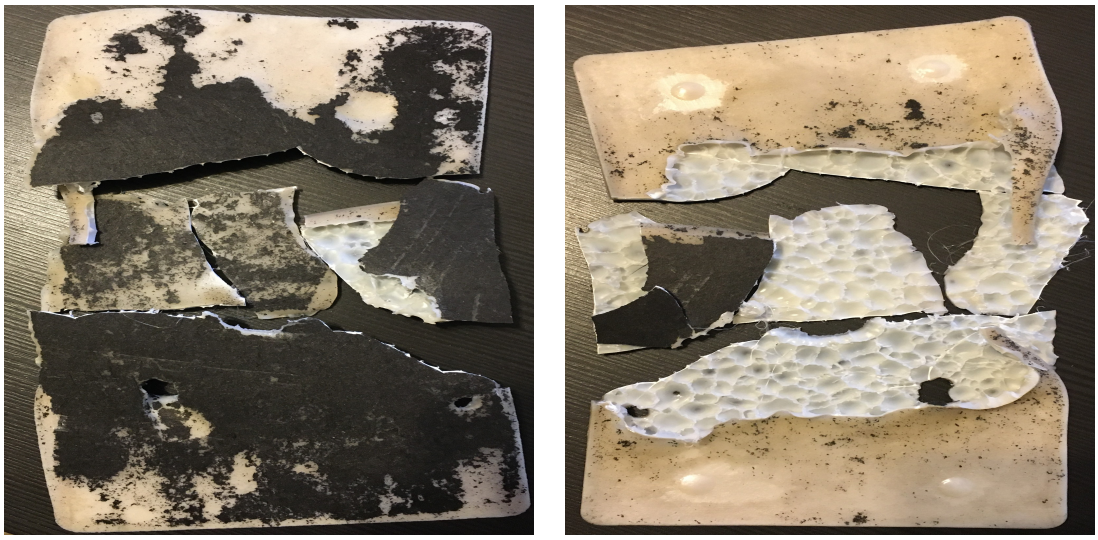

(a) Front View (b) Rear View

Figure 5.2: Trial One with CBAM Mold Plates

5.2.1. First Trial. The first trial created an ABS part with a cooling time of approximately 30 seconds. However, the part failed to solidify properly within the allotted cooling time. Additionally, the adhesion at the ABS and tooling surface interface was large enough that when the clamping unit disengaged and opened the mold, the structural integrity of the part failed and tore into several pieces. These pieces had to be physically removed from the tooling surface of both CBAM mold plates, which proved to be a difficult task due to high adhesion. Upon removal, portions of the PEEK binding matrix of the CBAM mold plates were removed and seen on the exterior surface of the ABS part. Figure 5.2b displays improper solidification of the interior of the ABS part, which contributed to the part's inability to withstand structural failure upon the opening of the mold cavity. Due to the tooling surface degradation and structural failure of the part, the process was discontinued for further analysis and resumed the following day.

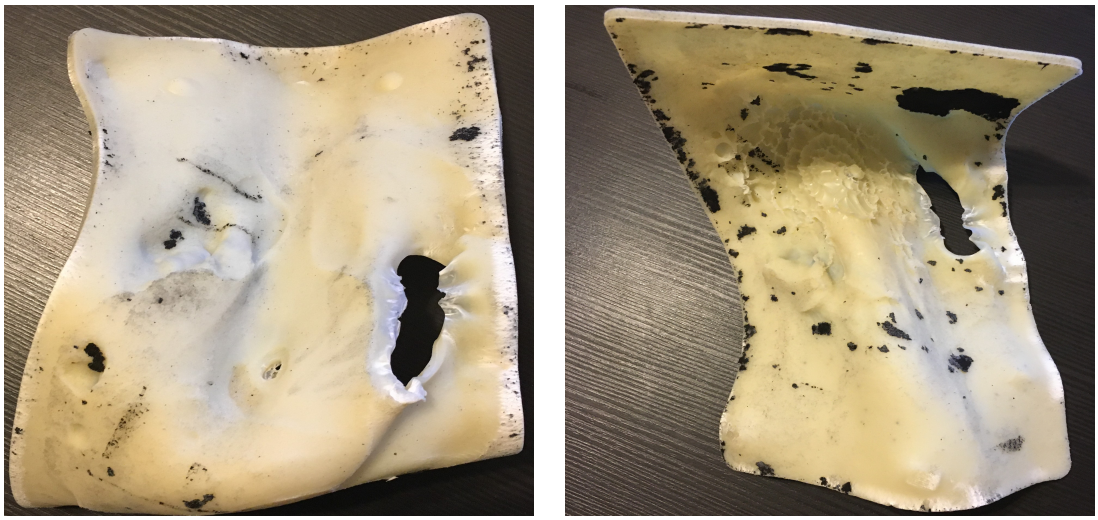

(a) Front View (b) Rear View

Figure 5.3: Trial Two with CBAM Mold Plates

5.2.2. Second Trial. Since the allotted cooling time from the first trial failed to provide sufficient part solidification, the cooling time was increased to 60 seconds. Additionally, in order to avoid further removal of the PEEK matrix and degrading the tooling surface of the CBAM mold plates, five layers of mold release were applied over a span of 1 hour and 15 minutes. One key observation was that the mold release appeared to be absorbed by the matrix of the mold plates. The PEEK binding matrix has a porosity present, so this is a probable cause for why the mold release did not appear to completely remain on the tooling surface. However, the injection molding cycle was initiated. Figure 5.4 above displays a more intact, solidified ABS part after increasing the cooling time. The part extracted considerably less PEEK matrix from the tooling surface of the CBAM mold plates as well. Notice that the part appears to have experienced severe warping. The reasoning is two fold: first, the ABS had only cooled to a softening point after the cooling cycle and had not completely solidified; second, the part was not as warped as the images display until after the operator mechanically strained the part while trying to remove the part from the mold cavity. While the second trial was an improvement from the first trial, the cooling time parameters still needed adjustment.

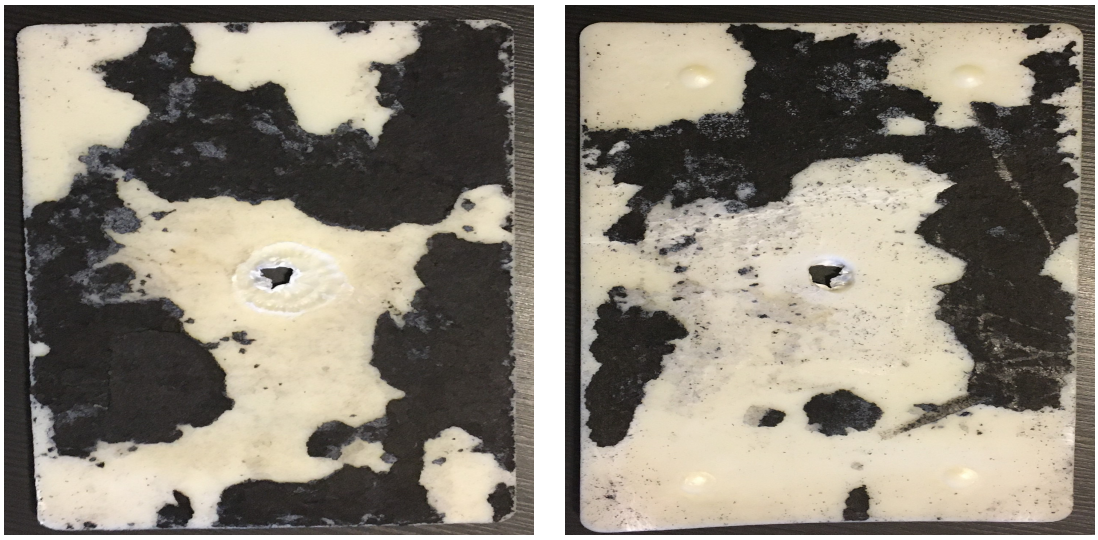

(a) Front View (b) Rear View

Figure 5.4: Trial Three with CBAM Mold Plates

5.2.3. Third Trial. After the second trial, the next shot was created and the injection molding cycle was repeated to initiate the third trial. Previously, the trials were unsuccessful, but demonstrated improvement with an increase in cooling time. In order to demonstrate that a part could be successfully injection molded with CBAM mold plates the cooling time was increased to 180 seconds. After running the third trial, the part was successfully created with only a few caveats. The part still demonstrated great adhesion to the CBAM mold plate tooling surface. Portions of the PEEK matrix were removed from the tooling surface just as the previous trials demonstrated. Also, the middle of the plate contains a hole. There are a couple of reasons this hole is present. One reason is that the heated sprue bushing keeps this region at 485°F, which keeps the polymer in a molten state. This is a consequence of the design of the current installed die and cannot be modified. Second, one of the five ejector pins that remained in the injection molding die after the installation of the CBAM mold plates happened to be located in the exact same region $\frac{1}{8}$ in. away from the heated sprue bushing. So, when the clamping unit opened the mold cavity and engaged the hydraulic eject cylinder to actuate the knockout bar, the ejector pin simply punched a hole right

through the unsolidified ABS. The one ejector pin in these trials demonstrated a lack of purpose and should have been removed with the others.

5.3. AFTERMATH

Following the third trial of the ABS part manufacturing the CBAM mold plates were examined. The tooling surfaces of the static and dynamic mold plates experienced noticeable degradation. In order to prevent further damage to the tooling surfaces, additional experimental trials for the study were discontinued. Simulation software was then implemented for further analysis of the CBAM mold plates and ABS part. Figure 5.5 and Figure 5.6 shows the tooling surfaces of the static and dynamic CBAM mold plates, respectively, before and after the trials.

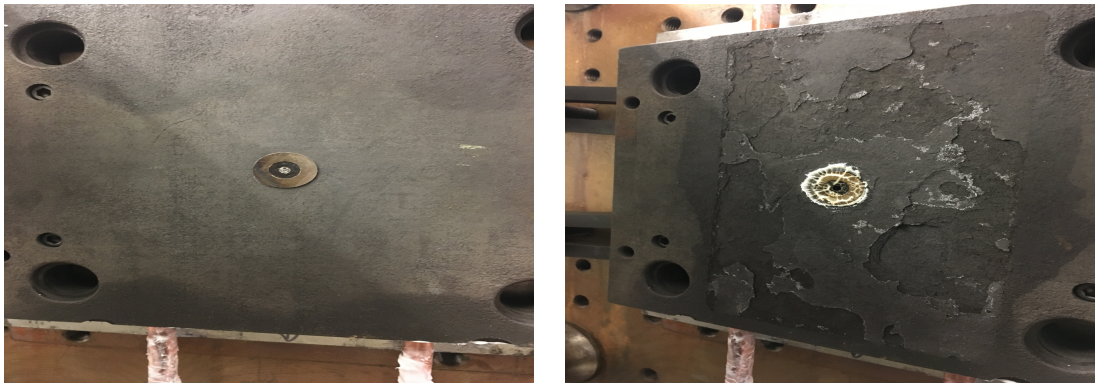

(a) Before Trials (b) After Trials

Figure 5.5: Static CBAM Mold Plate

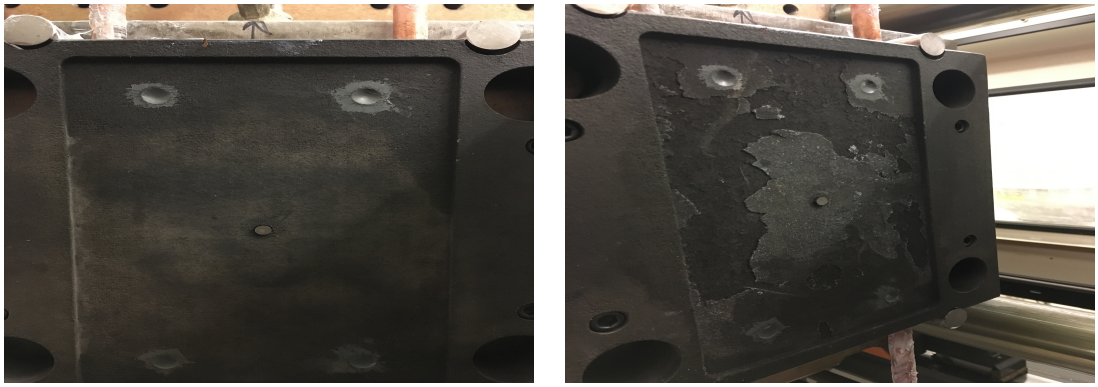

(a) Before Trials (b) After Trials

Figure 5.6: Dynamic CBAM Mold Plate

6. SIMULATION

6.1. PMMA AND P20 STEEL EXAMPLE

Software packages, such as Solidworks Plastics, were utilized for simulation analysis in this research. Solidworks Plastics contains a large database with commonly processed plastics, metal molds, and their respective material properties [23]. These materials for the polymer and molds produce reasonably accurate results via finite element methods. An initial validation run of the simulation below was conducted for polymethylmethacrylate (PMMA) polymer processed in a P20 steel mold. The fill–time results from the simulation were compared to the part created via the injection molding process and are displayed in Figure 6.1 below.

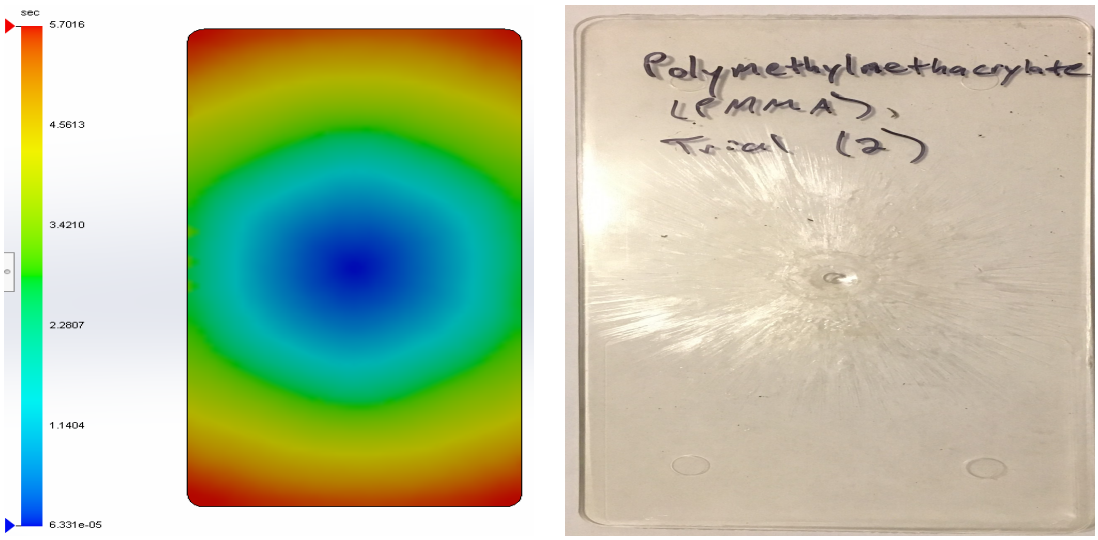

(a) PMMA Simulation (b) PMMA Experiment

Figure 6.1: Fill Time Simulation vs Experiment for PMMA

For the comparison above, the PMMA part was created first and found experimentally to take 6 seconds to fully fill the mold cavity. Using the same set of parameters, the simulation software predicted the fill time to be approximately 5.7 seconds. To further validate the fill time with the part results, a short shot was experimentally induced with a fill time of 3.5 seconds. Simulation results injected

the same amount of molten PMMA in 3.37 seconds. The comparison in Figure 6.2 below shows the amount of material processed in simulation and experiment.

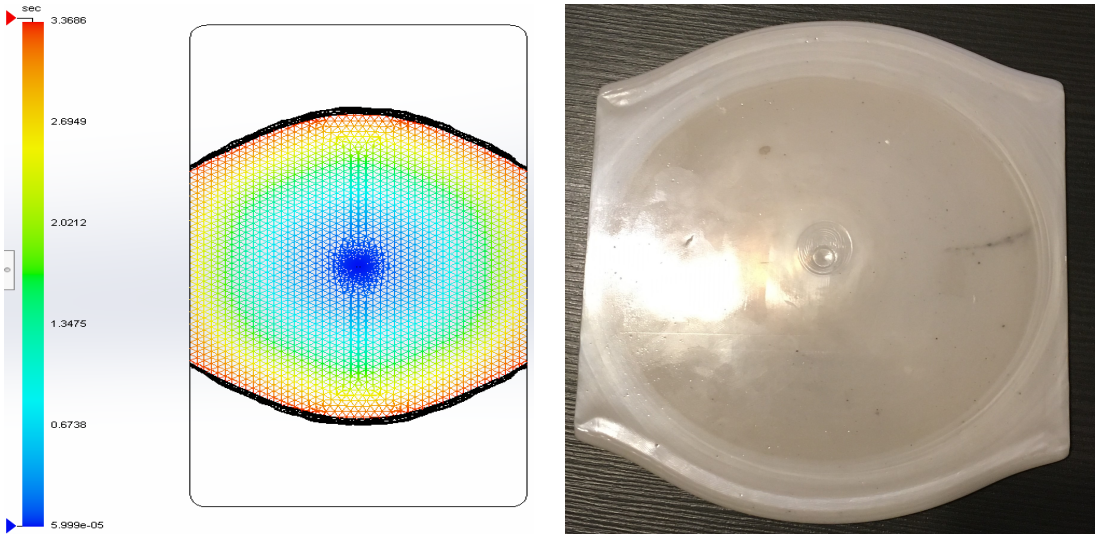

(a) PMMA Simulation Short Shot (b) PMMA Experiment Short Shot

Figure 6.2: Fill Time Simulation vs Experiment for PMMA Short Shot

6.2. ABS AND CARBON FIBER/PEEK EXAMPLE

6.2.1. Computer-Aid Design Modeling. This same approach of comparing simulation with experimentation was attempted for ABS and the carbon fiber/PEEK mold plates in this research. First, the dimensions of the part were drawn in the Solidworks CAD modeling software [14]. After the part's shape was developed, the Solidworks Plastics software was accessed [23]. The procedure for developing the finite element model via Solidworks Plastics was similar to other finite element softwares.

6.2.2. Finite Element Analysis. The boundary conditions required an injection location. The center of the part was the selected injection location for this study. The sprue bushing injection diameter was initialized to $\frac{1}{8}$ in. Next, the boundary condition for the mold wall temperature was established. The entire part was selected and the mold wall temperature was initialized to 100°F.

After the boundary conditions were established, a three-dimensional, solid meshing procedure for the part was performed. Depending on the complexity of the mold, several domain types may need to be selected for meshing. However, for this study the entire cavity was the part volume; therefore, the domain type for the part shape was cavity. Following the domain selection was the creation of the surface mesh. For this study, the only domain was the cavity. The cavity was selected and the surface element shape was an $\frac{1}{8}$ in. side length, equilateral triangle. The number of present triangular elements for this surface mesh was $15,577$. As a result, there were $27,612$ tetrahedral elements implemented in the total mesh as a result of the surface meshing. Since the element size was sufficiently small and the part geometry was simple, no local refinement was assigned. The part was then meshed with smooth gradation. Notice that the software induced bias near the injection site. This was important as the thermal gradient in the part would be likely highest at this location; the deviations in the flow models would be most drastic within this region. A summary of the solid mesh appeared. Provided that the summary passed the program's and user's satisfactions, the meshing sequence proceeded; otherwise, the previous parameters were altered until satisfaction was met. There were additional tools in the proceeding interface for customizing the mesh. These tools were not needed for this study. Next, the solid mesh was created with a tetrahedral solid mesh type for consistency. However, immediately after this selection, the hybrid mesh type was applied in order to allow the meshing sequence to appropriately construct the surface and solid meshes, especially within regions where bias was induced. The mesh size selected was .0039 in. for the element side length. Again, a smooth gradation for the mesh transition was selected. The solid mesh was then created. The remaining meshing tools were not necessary for this study and were skipped. This concluded the meshing sequence.

Following the meshing sequence came the material selections for the polymer and the mold. Solidworks Plastics provided a plethora of industrial materials and numerous variations with defined material parameters to create accurate and precise injection molding simulations. However, this section required user input that came with a caveat that needed to be emphasized for this study. While Lustran 348 ABS could easily be accessed from the default database, there were no carbon fiber/PEEK mold material parameters present; these parameters needed to be defined by the user. The caveat was that the mold material parameters provided for user input were programmed for isotropic materials. This did not come as a surprise since this research was aimed at breaking ground for CBAM implementation into the injection molding process. Unfortunately, there did not appear to be any subroutine implementation methods provided in Solidworks Plastics at that time. So, accuracy was sacrificed. After consulting the company sponsoring this research, the conclusion was made to use the through-thickness properties over planar properties when necessary. Table 2.2 provided the mold material parameters for carbon fiber/PEEK used in this simulation. Additional CBAM mold material parameters needed were the specific heat, $.363\frac{BTU}{lb_m{}^\circ F}$ and the shear modulus, 4.8258 GPa.

Now, the injection molding processing parameters needed to be defined. For this research, many of the cycle time parameters were found via trial and error and not necessarily by analytical means. The first sequence performed during the injection process, following the shot, was the filling sequence. The filling sequence parameters are provided in Table 6.1 below.

Table 6.1: Filling Sequence Parameters

Filling Process Parameters		
Filling Time	6	(s)
Melt Temperature	485	(°F)
Mold Temperature	100	(°F)
Injection Pressure Limit	27	(ksi)
Clamp Force Limit	165	(tons)

Next, the packing sequence parameters are displayed for this study in Table 6.2 below.

Table 6.2: Packing Sequence Parameters

Packing Sequence Parameters		
Pressure Holding Time	1	(s)
Pure Cooling Time	180	(s)

Finally, the warping settings were initialized to the ambient temperature, which was 68°F in this case. At that point, the setup to run the finite element analysis was prepared. The literature advises the user to run analyses for flow, packing, and warping. Then the results from the simulation may be viewed for post-processing.

While the simulation results conducted here for this study contain a degree of error, the data may serve provisional insight for what future researchers may expect to find from the injection molding cycle using CBAM mold plates.

From Figure 6.3a the simulation calculated a filling cycle time of approximately 5.83 seconds. The user found from experiment that 6 seconds sufficiently filled the mold cavity without leaving any residual flashing on the part. However, the simulation cooling cycle time appeared to be significantly lower than the experiment. The most likely reason for the large difference in cycle times may be that the simulation was not accounting for the heated sprue bushing located in direct contact with the part, even if its location was relatively close to the mold cavity.

In the experiment, the heated sprue bushing was keeping the local temperature near the injection site at approximately 485°F.

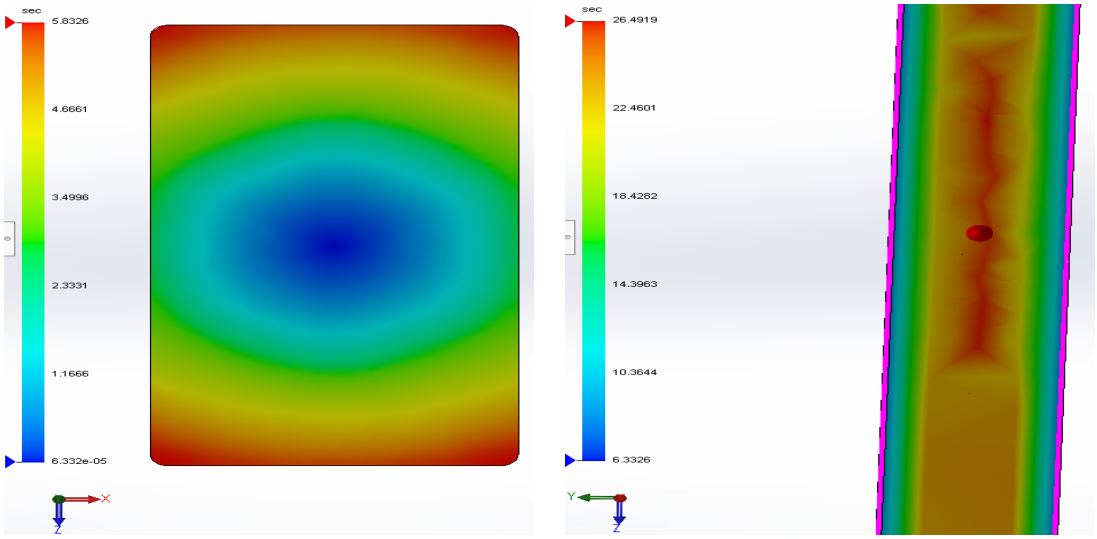

(a) Cycle Filling Time (b) Cycle Cooling Time

Figure 6.3: ABS Cycle Time Analytics from Simulation

Next, Figure 6.4 displayed the temperature and pressure analytics at the end of the filling and cooling cycles. Figure 6.4b displayed important information that, even if the values were slightly off, could be verified during the CBAM injection molding trials. The glass transition temperature for ABS, T_g, is approximately 105°C [7, 19, 20]. Following the finite element simulation, the temperature at the end of the cooling cycle showed that the hottest element in the part was below the glass transition temperature for ABS. Therefore, the part had gained rigid mechanical properties at that point and did not display soft, flexible characteristics. More important information was displayed in Figure 6.4a. This image displayed the temperature profile at the end of the filling cycle. This thermal distribution provided could inform the injection molding operator if a material, especially those that are semi-crystalline, may fall below the melt temperature, T_m.

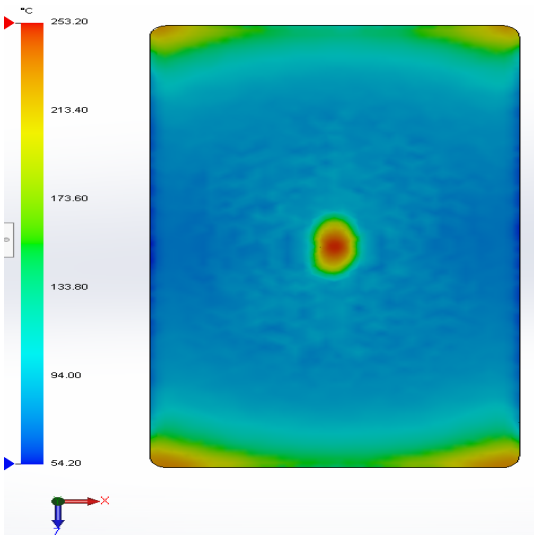

(a) End Fill Temperature

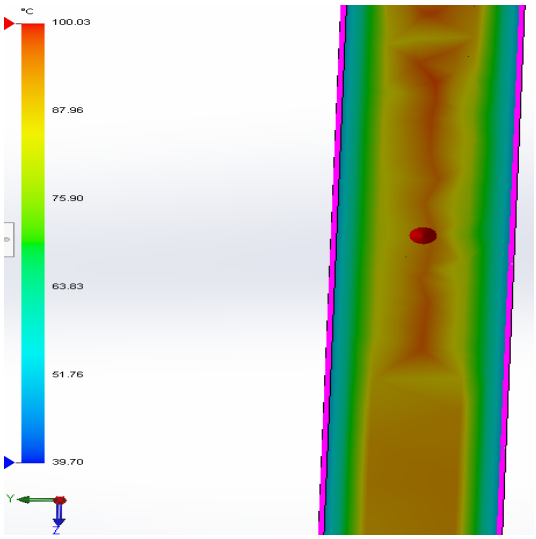

(b) End Cooling Temperature

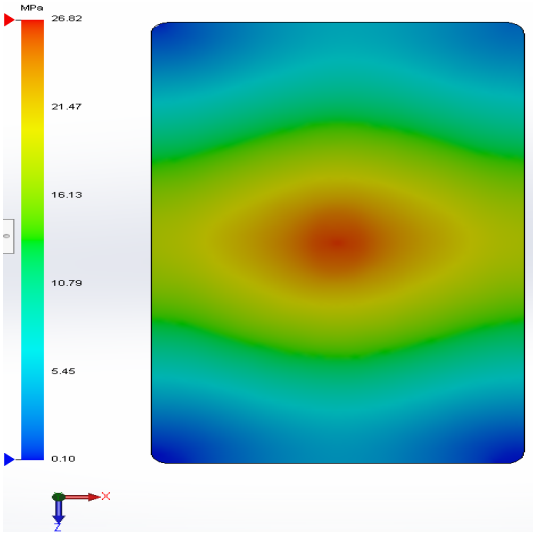

(c) End Fill Pressure

Figure 6.4: ABS Temperature and Pressure Analytics from Simulation

Crystallization may begin for semi-crystalline structures if the polymer drops below the melt temperature during the fill cycle [1]. In the injection molding process, crystallization is likely to occur because the thermal gradient that exists between the polymer/mold interface is too large [16]. Decreasing the thermal gradient can prevent early onset of crystallization during the filling sequence. This is one of the main reasons why injection molding plates are initially heated to a specific temperature. For example, PMMA displays transparency when processed appropriately. However, the transparency property can be substantially

altered if the thermal gradient between the polymer and the mold is sufficiently large. Figure 6.5 below displays the effects of decreasing the thermal gradient or increasing the mold temperature. Figure 6.5a displays the effect of a large thermal gradient and produces the least amount of transparency in the PMMA part. As the mold temperature is increased, the transparency of the PMMA parts are increased. Figure 6.5c displays some crystallization near the injection region where the thermal gradient was largest during the filling cycle. However, the increase in transparency is demonstrated here by increasing the mold temperature prior to injection.

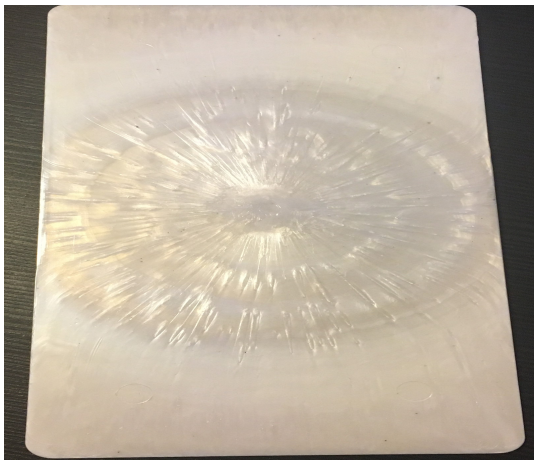

(a) Opaque PMMA Part

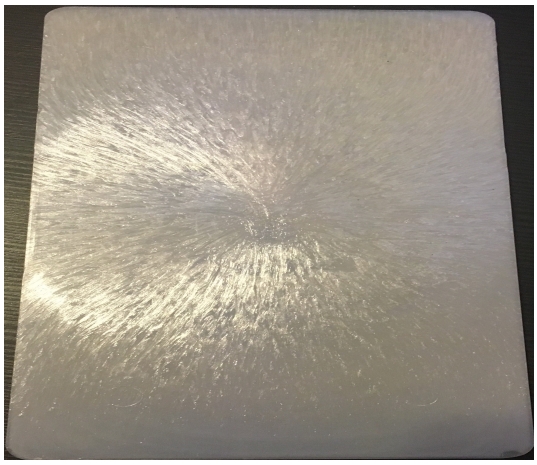

(b) Translucent PMMA Part

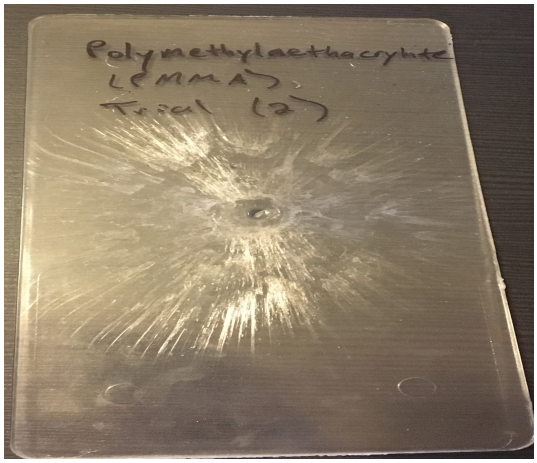

(c) Transparent PMMA Part

Figure 6.5: Transparency Comparison of PMMA Parts

Shrinkage is an effect that occurs throughout the injection sequence. Figure 6.6a displays regions of the part at the end of the filling sequence where volumetric shrinkage is largest. Notice that volumetric shrinkage appears to occur most severely in regions where the temperature profile is highest. The shrinkage effect necessitates the packing sequence to help refill the entire cavity after the filling sequence. Notice the volumetric shrinkage in Figure 6.6b at the end of the packing sequence is less drastic than at the end of the filling sequence.

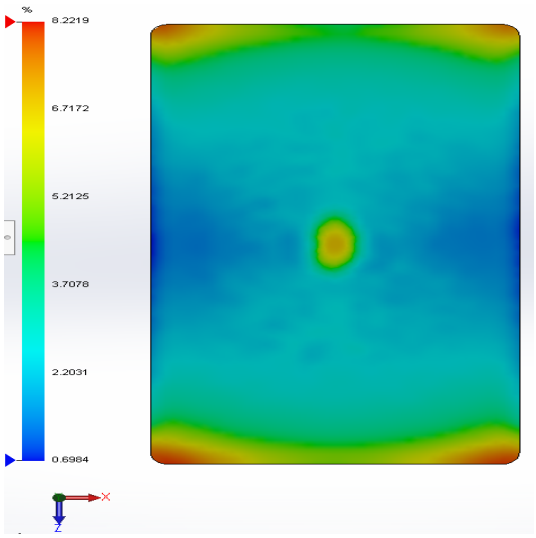

(a) End of Fill Volumetric Shrinkage

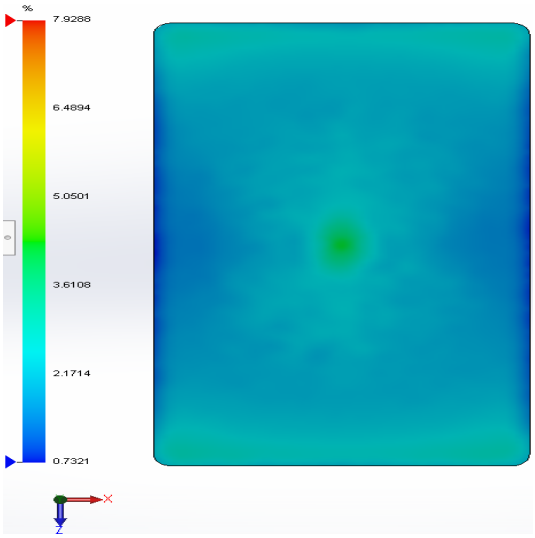

(b) End of Packing Volumetric Shrinkage

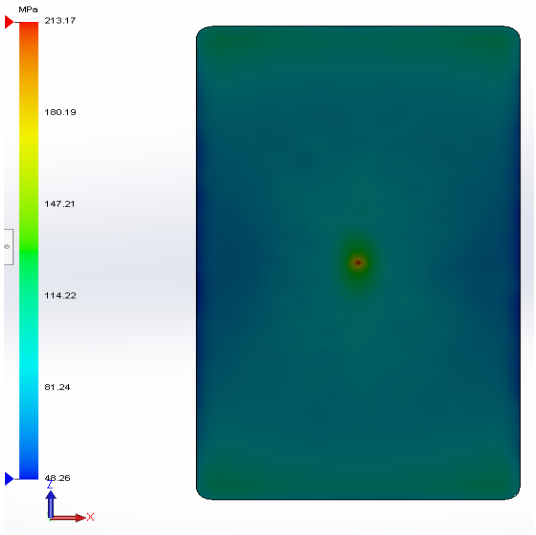

(c) Residual Stress

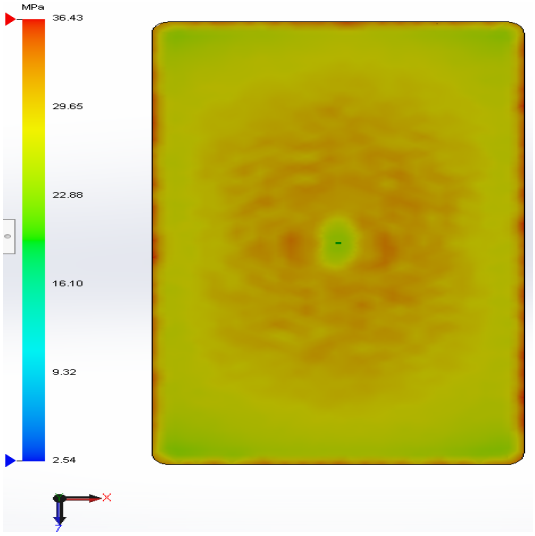

(d) In Mold Residual von Mises Stress

Figure 6.6: ABS Stress and Shrinkage Analytics from Simulation

Figure 6.6c and Figure 6.6d display the residual and von Mises stress distributions, respectively, of the part. The residual stresses induced during the polymer injection molding cycle can be reduced with longer cooling times. Low cooling times result in ejecting the part sooner. This process exposes the part to the atmospheric temperature, which is most often lower than the mold plate temperature, and will likely induce greater warping effects. Minimizing warping is critical, especially in parts that require accuracy and precision. For example, pharmaceutical companies need prescription containers and lids to fasten together properly. Polymer warping from residual stresses may misalign the threading of the lid and container and produce difficulty in properly sealing the product inside. Figure 6.7 displays the total stress displacement and the components of stress displacement along the x, y, and z axes. Note that the polymer initially flows along the positive y axis at the injection site. Each figure displayed in the Simulation section faces the negative y direction, except for Figure 6.6c.

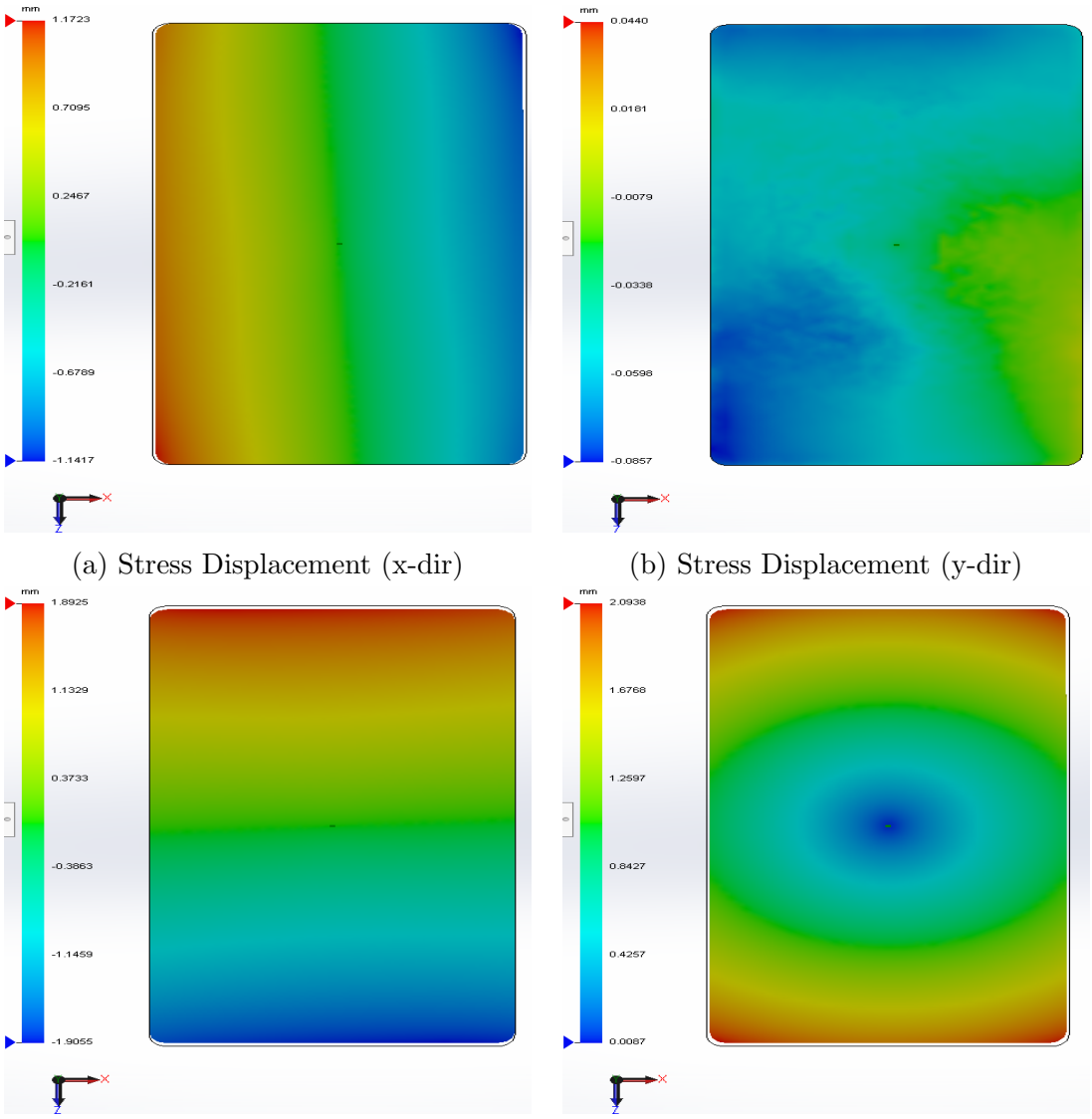

(a) Stress Displacement (x-dir)

(b) Stress Displacement (y-dir)

(c) Stress Displacement (z-dir)

(d) Total Stress Displacement

Figure 6.7: ABS Warping Analytics from Simulation

7. CONCLUSIONS

7.1. RESULTS

CBAM injection molding plates have potential to replace metal injection molding plates for relatively small cycle productions. After conducting a few trials with the carbon fiber/PEEK injection molding plates used in this study, a part was successfully created. The geometry of the part was the same as those created within the metal mold. Additionally, the shrinkage and warping effects appeared to be consistent with parts made via the metal mold plates. The cooling cycle time for the parts made from the CBAM mold plates was substantially longer than those of the metal mold plates though. However, the tooling surface of the CBAM mold plates was noticeably degraded after each trial. Specifically, the PEEK matrix of the tooling surface was torn due to the high adhesion between the ABS/PEEK interface. This made part ejection difficult and required the user to forcefully remove the part from the mold. Mold removal appeared to have little effect on the CBAM mold plates; the matrix appeared to absorb the mold removal within the mold plates' porosity. The surface finish of the part contained the removed regions of PEEK material from the CBAM mold plates. The surface area of the parts that did not contain PEEK material exhibited a rougher surface finish than parts created in metal molds. However, post-processing methods can smooth the surface to be similar to parts made in metal molds. Lastly, the reduction in cost for fabricating mold plates via the CBAM method is a fraction of the expense that arises from subtractive manufacturing of metal mold plates. While there are manufacturing and engineering modifications that need to be made for better quality part production with CBAM mold plates, there is certainly purpose, direction, and motivation for successfully replacing metal molds with CBAM molds.

7.2. RECOMMENDATIONS

7.2.1. Plate Manufacturing. The CBAM method in this study used transversely isotropic carbon fiber sheets with PEEK matrix. This additive manufacturing method does not allow for empty spaces within the working plane, such as holes that might be used for cooling lines. Modifications made to the plates prior to shipment experienced thermal shrinkage that caused critical components, such as ejector pins, pinions, and fastening components, to align improperly. Therefore, modifications to the injection molding die had to be made in order to properly fasten the composite plates to the die. One recommendation for future production may be to print the outline of the part from the build block without any modifications. Once the part arrives at the location, the machinist can visually compare the mold plates to the injection molding die and determine the precise measurements needed in order to reduce human error. This may also help to reduce the amount of machining modifications made to the metal die, which will save time and cost.

Another recommendation for producing CBAM mold plates would be to apply an epoxy/resin to the tooling surface in order to reduce the porosity. This will help to eliminate the mold plate from absorbing any mold release agents. In fact, if the surface is sufficiently smooth the necessity for mold release may be eliminated altogether. However, the epoxy/resin will need to be able to withstand the thermal and pressure limits induced during the injection sequence. One proposed way to bypass this altogether is to cover the tooling surface with a metallic sheet. After the part is created, the sheet would simply be removed along with the part. This may work well with simple geometries, such as the rectangular prism part used in this research. For more complex molds, this method may prove difficult to implement. Combining both previous proposed solutions, the CBAM mold plates could be metal plated on the tooling surfaces.

7.2.2. Education. The author highly advises that any individual interested in pursuing research with polymers take courses in polymer science and conduct extensive literature searches prior to beginning any serious research endeavors. Eliminating ignorance will save a lot of time and stress.

7.3. FUTURE RESEARCH AND DEVELOPMENT

After the recommendations are applied, future research should investigate part production with carbon fiber/PEEK molds and increasing the longevity of the tooling surfaces. Once this is accomplished, other composite materials should be integrated into the CBAM manufacturing process for injection molding applications. Varying the composites can provide insight into the most appropriate materials for injection molding applications. Furthermore, the CBAM process should be integrated and analyzed in other manufacturing applications, such as compression molding.

Analytical calculations requiring an integrated understanding of polymer science should be performed to determine cycle time parameters. These parameters should be implemented in both simulation and in the injection molding machine. The outcomes of both processes should be compared to determine precision and accuracy of the analytics.

Rheological studies should be thoroughly conducted among amorphous and semicrystalline polymers in order to analyze non-Newtonian flow characteristics, which will increase the precision of the cycle time calculations.

After parts are made, coupons should be cut from these parts. These coupons should be tested for mechanical properties and compared to parts made from metal molds. If the cooling times are the same, then the quality of the parts will differ and so will the mechanical properties.

BIBLIOGRAPHY

[1] Shrivastava, A., 2018, Introduction to plastics engineering, William Andrew, Oxford, United Kingdom., pp. 17-48, 143-177.

[2] Kerkstra, R., and Brammer, S., 2018, Injection molding advanced troubleshooting guide, Hanser Publications, Cincinnati., pp. 125-130, 377-393, 457-468.

[3] Impossible Objects, 2021, Introduction to the Impossible Objects CBAM 2 Printer, Version 1.07, United States of America, Confidential Document.

[4] n.d. Injection Molding Machine User's Manual. 1st ed. Batavia: Cincinnati Milacron, pp.V2-V3, VI1-VI3, VII1-VII3, VIII1-VIII4.

[5] Prototech Asia, 2018, Injection Molding Machine Layout. Available: https://prototechasia.com/en/injection-molding/stages-injection-molding.

[6] García, M., Schlatter, M., Cabrera, F., Manzanares, J., and Hanafi, I., 2016, "Recycling of Acrylonitrile–Butadiene–Styrene Using Injection Moulding Machine," Procedia Technology, 22, pp. 399-406.

[7] 2021, "Acrylonitrile Butadiene Styrene (ABS Plastic): Uses, Properties & Structure", Omnexus.specialchem.com. Available: https://omnexus.specialchem.com/selection-guide/acrylonitrile-butadiene-styrene-abs-plastic.

[8] Hudson Tool Steel Corporation, "P20 Mold Steel Technical Data," 2021. Available: https://www.hudsontoolsteel.com/technical-data/steelP0.

[9] Impossible Objects, 2020, "Game Changing Materials for Real-World Composite Parts."

[10] Impossible Objects, 2017, "ASTM D5470 Thermal Transmission Testing," Composites Innovation Centre, Private and Confidential Document.

[11] Impossible Objects, 2017, "ASTM E831 CTE Testing," Composites Innovation Centre Private and Confidential Document.

[12] JB Weld, 2018, "Steel Reinforced Epoxy Resin Data," Available: https://www.jbweld.com/product/j-b-weld-twin-tube.

[13] Rex Plastics, 2013, "How much does plastic injection molding cost?" Available: https://rexplastics.com/plastic-injection-molds/how-much-do-plastic-injection-molds-cost.

[14] SolidWorks, 2019, Dassault Systemes.

[15] Gibson, R., 2016, Principles of Composite Material Mechanics, CRC Press, Boca Raton., pp. 69-93, 193-207, 249-270, 350-353, 404-410.

[16] Yang, Y., Chen, X., Lu, N., and Gao, F., 2016,
Injection molding process control, monitoring, and optimization,
Hanser Publications, Cincinnati., pp. 1-38.

[17] Sorokina, S., and Romanov, A., 2018,
"Corrosion of Molds in Injection Molding Machines,"
Russian Engineering Research, 38(12), pp. 996-999.

[18] Corrosionpedia, 2014, Galvanic Series.
Available: https://www.corrosionpedia.com/an-introduction-to-the-galvanic-series-galvanic-compatibility-and-corrosion/2/1403.

[19] Ineos Styrolution, "Lustran 348 Acrylonitrile Butadiene Styrene Technical Datasheet," n.d.[Revised Jan. 2016]. Available: http://www.ineos-styrolution.com/.

[20] Fast Heat, "ABS (Acrylonitrile-Butadiene-Styrene)," n.d.[Revised Mar. 2014].
Available: http://www.fastheatuk.com/mdb/abs.html.

[21] K and S Precision Metals and Mueller Industries,
"Tubing and Pipe Fittings," 2020, Grainger.

[22] Colmenero, J., Lazaro, M., Donate, C., Paramio, M., Idoipe, A.,
Garcia, J., Sevillano, J., and Puerto, D., 2016,
"Analytical calculation model for determining the cycle time in injection molding parts applied to design optimization algorithms",
High Performance and Optimum Design of Structures and Materials,
166(1743-3509), pp. 427-434.

[23] SolidWorks Plastics, 2019, Dassault Systemes.

VITA

Cody Bivens was born on a military installation in the United States of America. He completed the requirements for the bachelor's of science degree in aerospace engineering in 2019, as well as the requirements for the master's of science degree in aerospace engineering in May 2021. Both degree programs were completed at the Missouri University of Science and Technology.